39. Aigner S, Lingner J, Goodrich KJ, Grosshans CA, Shevchenko A, et al. (2000) Euplotes telomerase contains an La motif protein produced by apparent translational frameshifting. EMBO J 19: 6230–6239. PubMed: 11080168.
40. Das S, Ott M, Yamane A, Tsai W, Gromeier M, et al. (1998) A small yeast RNA blocks hepatitis C virus internal ribosome entry site (HCV IRES)-mediated translation and inhibits replication of a chimeric poliovirus under translational control of the HCV IRES element. J Virol 72: 5638–5647. PubMed: 9621022.
41. Kim YK, Back SH, Rho J, Lee SH, Jang SK (2001) La autoantigen enhances translation of BiP mRNA. Nucleic Acids Res 29: 5009–5016. doi:10.1093/nar/29.24.5009. PubMed: 11812831.
42. Gauss-Müller V, Kusov YY (2002) Replication of a hepatitis A virus replicon detected by genetic recombination in vivo. J Gen Virol 83: 2183–2192. PubMed: 12185272.
43. Nakatake M, Monte-Mor B, Debili N, Casadevall N, Ribrag V, et al. (2012) JAK2(V617F) negatively regulates p53 stabilization by enhancing MDM2 via La expression in myeloproliferative neoplasms. Oncogene 31: 1323–1333. doi:10.1038/onc.2011.313. PubMed: 21785463.
44. Hsu S, Dickinson DP, Qin H, Lapp C, Lapp D, et al. (2005) Inhibition of autoantigen expression by (-)-epigallocatechin-3-gallate (the major constituent of green tea) in normal human cells. J Pharmacol Exp Ther 315: 805–811. doi:10.1124/jpet.105.090399. PubMed: 16046615.
45. Wang Q, Liu Y, An D, Diao H, Xu W, et al. (2012) Regulation of hepatitis C virus translation initiation by iron: role of eIF3 and La protein. Virus Res 167: 302–309. doi:10.1016/j.virusres.2012.05.014. PubMed: 22634302.
46. Tang J, Huang ZM, Chen YY, Zhang ZH, Liu GL, et al. (2012) A novel inhibitor of human La protein with anti-HBV activity discovered by structure-based virtual screening and in vitro evaluation. PLoS One 7: e36363. doi:10.1371/journal.pone.0036363. PubMed: 22558448.
47. Meydan N, Grunberger T, Dadi H, Shahar M, Arpaia E, et al. (1996) Inhibition of acute lymphoblastic leukaemia by a Jak-2 inhibitor. Nature 379: 645–648. PubMed: 8628398.
48. Okitsu K, Kanda T, Imazeki F, Yonemitsu Y, Ray RB, et al. (2010) Involvement of interleukin-6 and androgen receptor signaling in pancreatic cancer. Genes Cancer 1:859–867. doi:10.1177/1947601910383417. PubMed: 21779469.
49. Duan Z, Bradner JE, Greenberg E, Levine R, Foster R, et al. (2006) SD-1029 inhibits signal transducer and activator of transcription 3 nuclear translocation. Clin Cancer Res 12: 6844–6852. doi:10.1158/1078-0432.CCR-06-1330. PubMed: 17121906.
50. Goswami BB, Kulka M, Ngo D, Cebula TA (2004) Apoptosis induced by a cytopathic hepatitis A virus is dependent on caspase activation following ribosomal RNA degradation but occurs in the absence of 2′-5′ oligoadenylate synthetase. Antiviral Res 2004 63:153–166. doi:10.1016/j.antiviral.2004.02.004. Pub Med: 15451183.
51. Basu A, Meyer K, Ray RB, Ray R (2001) Hepatitis C virus core protein modulates the interferon-induced transacting factors of Jak/Stat signaling pathway but does not affect the activation of downstream IRF-1 or 561 gene. Virology 288:379–390. PubMed: 11601909.
52. Rosenthal A, Mesa RA (2014) Janus kinase inhibitors for the treatment of myeloproliferative neoplasms. Expert Opin Pharmacother [Epub ahead of print]. doi:10.1517/14656566.2014.913024. PubMed: 24766055.
53. Gonzales AJ, Bowman JW, Fici GJ, Zhang M, Mann DW, et al. (2014) Oclacitinib (APOQUEL®) is a novel Janus kinase inhibitor with activity against cytokines involved in allergy. J Vet Pharmacol Ther [Epub ahead of print]. doi:10.1111/jvp.12101. PubMed: 24495176.
54. Cutolo M, Meroni M (2013) Clinical utility of the oral JAK inhibitor tofacitinib in the treatment of rheumatoid arthritis. J Inflamm Res 6: 129–137. doi:10.2147/JIR.S35901. PubMed: 24453498.
55. Kanda T, Imazeki F, Yokosuka O (2010) New antiviral therapies for chronic hepatitis C. Hepatol Int 4: 548–561. doi:10.1007/s12072-010-9193-3. PubMed: 21063477.
56. Robertson BH, Jansen RW, Khanna B, Totsuka A, Nainan OV, et al. (1992) Genetic relatedness of hepatitis A virus strains recovered from different geographical regions. J Gen Virol 73: 1365–1377. PubMed: 1318940.
57. Zeisel MB, Lupberger J, Fofana I, Baumert TF (2013) Host-targeting agents for prevention and treatment of chronic hepatitis C - perspectives and challenges. J Hepatol 58: 375–384. doi:10.1016/j.jhep.2012.09.022. PubMed: 23041307.
58. Kiyohara T, Totsuka A, Yoneyama T, Ishii K, Ito T, et al. (2009) Characterization of anti-idiotypic antibodies mimicking antibody- and receptor-binding sites on hepatitis A virus. Arch Virol 154: 1263–1269. doi: 10.1007/s00705-009-0433-6. PubMed: 19578927.
59. Casas N, Amarita F, de Marañón IM (2007) Evaluation of an extracting method for the detection of Hepatitis A virus in shellfish by SYBR-Green real-time RT-PCR. Int J Food Microbiol 120: 179–185. PubMed: 17900731.

INAM Plays a Critical Role in IFN-γ Production by NK Cells Interacting with Polyinosinic-Polycytidylic Acid–Stimulated Accessory Cells

Jun Kasamatsu,* Masahiro Azuma,*,[1] Hiroyuki Oshiumi,* Yuka Morioka,[†] Masaru Okabe,[‡] Takashi Ebihara,*,[2] Misako Matsumoto,* and Tsukasa Seya*

Polyinosinic-polycytidylic acid strongly promotes the antitumor activity of NK cells via TLR3/Toll/IL-1R domain–containing adaptor molecule 1 and melanoma differentiation-associated protein-5/mitochondrial antiviral signaling protein pathways. Polyinosinic-polycytidylic acid acts on accessory cells such as dendritic cells (DCs) and macrophages (Mφs) to secondarily activate NK cells. In a previous study in this context, we identified a novel NK-activating molecule, named IFN regulatory factor 3–dependent NK-activating molecule (INAM), a tetraspanin-like membrane glycoprotein (also called Fam26F). In the current study, we generated INAM-deficient mice and investigated the in vivo function of INAM. We found that cytotoxicity against NK cell–sensitive tumor cell lines was barely decreased in *Inam*$^{-/-}$ mice, whereas the number of IFN-γ–producing cells was markedly decreased in the early phase. Notably, deficiency of INAM in NK and accessory cells, such as CD8α^{+} conventional DCs and Mφs, led to a robust decrease in IFN-γ production. In conformity with this phenotype, INAM effectively suppressed lung metastasis of B16F10 melanoma cells, which is controlled by NK1.1^{+} cells and IFN-γ. These results suggest that INAM plays a critical role in NK-CD8α^{+} conventional DC (and Mφ) interaction leading to IFN-γ production from NK cells in vivo. INAM could therefore be a novel target molecule for cancer immunotherapy against IFN-γ–suppressible metastasis. *The Journal of Immunology*, **2014, 193: 5199–5207.**

Microbial components play a major role in activating innate and adaptive immune responses by triggering pattern recognition receptors. Nucleic acid adjuvants, including polyinosinic-polycytidylic acid (polyI:C) and unmethylated CpG dinucleotides, strongly promote Th1 immune responses against cancer and infected cells and induce type I IFN and other inflammatory cytokines (1, 2). PolyI:C strongly enhances priming and expansion of Ag-specific T cells and NK cells with dramatic regression of syngeneic implant tumors in mice (3–6). NK cells belong to group 1 innate lymphocytes (ILC1s) and control progression of several types of tumors and microbial infections (7). Although polyI:C (an analog of viral dsRNA) is a ligand for multiple receptors, including dsRNA-dependent protein kinase, retinoic acid–inducible gene-I, melanoma differentiation–associated protein-5 (MDA5), and TLR3, both of the pathways initiated by TLR3/Toll/IL-1R domain–containing adaptor molecule 1 (TICAM-1) and MDA5/mitochondrial antiviral signaling protein confer antitumor activity on NK cells in vivo (8, 9).

PolyI:C also directly and indirectly activates human NK cells and other ILC1s (10, 11). PolyI:C participates in secondary activation of murine NK cells through stimulation of accessory cells such as dendritic cells (DCs) and other myeloid cells (12–14). In these interactions, previous studies have shown that type I IFN and cell contact via IL-15 receptors play a critical role in accessory cell activation followed by NK activation (15). In contrast, our previous studies showed that polyI:C induced bone marrow–derived DC (BMDC)–mediated NK cell activation through the TLR3/TICAM-1/IFN regulatory factor 3 (IRF3) pathway, which promoted antitumor immunity by adoptive transfer in a type I IFN- and IL-15–independent manner (8, 16). As the key molecule for this NK–DC interaction, we identified a novel IRF3-inducible tetraspanin-like membrane glycoprotein, named IRF3-dependent NK-activating molecule (INAM). INAM expression was induced not only in myeloid DCs but also in NK cells by polyI:C stimulation in vivo. Transfection of INAM in both BMDC and NK cells cooperated in inducing IFN-γ production and cytotoxicity against the NK-sensitive B16D8 cell line.

To investigate the role of INAM in vivo, we generated INAM-deficient mice by the standard gene-targeting method. INAM expression was induced not only in NK cells and conventional DC

*Department of Microbiology and Immunology, Graduate School of Medicine, Hokkaido University, Sapporo 060-8638, Japan; [†]Division of Disease Model Innovation, Institute for Genetic Medicine, Hokkaido University, Sapporo 060-8638, Japan; [‡]Research Institute for Microbial Disease, Osaka University, Osaka 565-0871, Japan

[1]Current address: Department of Pathology and Cellular Biology, Faculty of Medicine, University of Montreal, Montreal, QC, Canada.

[2]Current address: Department of Medicine, Howard Hughes Medical Institute, Washington University School of Medicine, St. Louis, MO.

Received for publication April 11, 2014. Accepted for publication September 9, 2014.

This work was supported in part by grants-in-aid from the Ministry of Education, Culture, Sports, Science and Technology and the Ministry of Health, Labor and Welfare of Japan, a Ministry of Education, Culture, Sports, Science and Technology of Japan Grant-in-Aid Project for Basic Research, "Carcinogenic Spiral," and the National Cancer Center Research and Development Fund (23-A-44). This work was also supported by the Takeda Science Foundation, the Yasuda Cancer Research Foundation, and the Iskra Foundation. J.K. is a Research Fellow of the Japan Society for the Promotion of Science.

Address correspondence and reprint requests to Prof. Tsukasa Seya, Department of Microbiology and Immunology, Graduate School of Medicine, Hokkaido University, Kita 15, Nishi 7, Kita-ku, Sapporo 060-8638, Japan. E-mail address: seya-tu@pop.med.hokudai.ac.jp

The online version of this article contains supplemental material.

Abbreviations used in this article: BMDC, bone marrow–derived DC; BST2, bone marrow stromal cell Ag 2; cDC, conventional DC; DC, dendritic cell; IFNAR1, IFN (α and β) receptor 1; ILC1, group 1 innate lymphocyte; INAM, IFN regulatory factor 3–dependent NK-activating molecule; IRF, IFN regulatory factor; Mφ, macrophage; MDA5, melanoma differentiation–associated protein-5; pDC, plasmacytoid DC; polyI:C, polyinosinic-polycytidylic acid; qPCR, quantitative real-time PCR; TICAM-1, Toll/IL-1R domain–containing adaptor molecule 1; WT, wild-type.

www.jimmunol.org/cgi/doi/10.4049/jimmunol.1400924

(cDC) subsets but also in other immune cells including macrophages (Mφs) and plasmacytoid DCs (pDCs) by polyI:C stimulation. Cytotoxicity against NK cell–sensitive tumor cell lines was barely decreased in *Inam*$^{-/-}$ mice, whereas the number of IFN-γ–producing cells markedly decreased in the early phase. We also showed that CD8α$^+$ cDCs and Mφs facilitate secretion of IFN-γ from NK cells in response to polyI:C stimulation in vitro and in vivo. Notably, deficiency of INAM on NK and their accessory cells led to a robust decrease in IFN-γ production. Therefore, these results infer that INAM plays a critical role in the interaction of NK-CD8α$^+$ cDCs (and Mφs) leading to IFN-γ production from NK cells. In agreement with this suggested phenotype, INAM effectively suppressed lung metastasis of B16F10 melanoma cells by controlling activation of NK1.1$^+$ cells and IFN-γ. Taken together, these results provide the first demonstration, to our knowledge, that INAM plays a critical role in the interaction of NK–CD8α$^+$ cDCs, which allows NK cells to produce IFN-γ. We propose in this study that INAM is a novel target molecule for immunotherapy against IFN-γ–suppressible tumors.

Materials and Methods

Mice

All mice were backcrossed with C57BL/6 mice more than seven times before use. A C57BL/6 background *Inam* (*Fam26f*)–targeted embryonic stem cell line, JM8A3.N1 of FAM26F tm2a (European Conditional Mouse Mutagenesis Program) Wtsi, was purchased from the European Conditional Mouse Mutagenesis Program. Chimeric mice were generated by aggregation of the mutated embryonic stem cells at the 8 cell stage. To remove exon 2 of *Inam*, the *Inam* heterozygous mutants were crossed with Cre-transgenic mice. The *Inam* heterozygous mutants obtained were intercrossed to obtain *Inam* homozygous mutants. *Ticam-1*$^{-/-}$ and *Mavs*$^{-/-}$ mice were generated in our laboratory (8, 16). *Irf-3*$^{-/-}$ and *Ifnar1*$^{-/-}$ mice were provided by Dr. T. Taniguchi (17). *Batf3*$^{-/-}$ C57BL/6 mice were purchased from The Jackson Laboratory (Bar Harbor, ME) (18). The *Batf3*$^{-/-}$ mice of C57BL/6 background [unlike 129 and BALB/c background (19)] lacked splenic CD8a$^+$ DCs as described previously (18) and evoked insufficient T cell functional response against extrinsic Ag and adjuvant (Azuma et al., submitted for publication). C57BL/6 background were purchased from CLEA Japan (Shizuoka, Japan). Experiments were performed with sex-matched mice at 8–14 wk of age. All mice were bred and maintained under specific pathogen-free conditions in the animal facility of the Hokkaido University Graduate School of Medicine. Animal experimental protocols and guidelines were approved by the Animal Safety Center, Hokkaido University.

Semiquantitative RT-PCR and quantitative real-time PCR

Total RNA was extracted using TRIzol according to the manufacturer's instructions (Invitrogen). cDNA was generated by using the High Capacity cDNA Transcription Kit (ABI) with random primers according to the manufacturer's instructions. Quantitative real-time PCR (qPCR) was performed using the Step One Real-Time PCR system (ABI). The primer sequences for qPCR analysis were 5′-CAACTGCAATGCCACGCTA-3′ and 5′-TCCAACCGAACACCTGAGACT-3′ for *Inam*; 5′-TTAACTGAGGCTGGCATTCATG-3′ and 5′-ACCTACACTGACACAGCCCAAA-3′ for *Il15*; 5′-GACAAAGAAAGCCGCCTCAA-3′ and 5′-ATGGCAGCCATTGTTCCTG-3′ for *Il18*; 5′-ACCGTGTTTACGAGGAACCCTA-3′ and 5′-GGTGAGAGCTGGCTGTTGAG-3′ for *Irf7*; 5′-GCCGAGACACAGGCAAAC-3′ and 5′-CCAGGGCTTGAGACACCTTC-3′ for bone marrow stromal cell Ag 2 (*Bst2*); and 5′-GCCTGGAGAAACCTGCCA-3′ and 5′-CCCTCAGATGCCTGCTTCA-3′ for *Gapdh*. The primer sequences for semi-qPCR analysis were 5′-CAACTGCAATGCCACGCTA-3′ and 5′-TCCAACCGAACACCTGAGACT-3′ for *Gapdh*.

Mφ depletion and stimulation using TLR agonists in vivo

To generate Mφ-depleted mice, mice were injected i.p. with 150 μl Clophosome-Clodronate Liposomes (FormuMax). For qPCR analysis of *Inam* induction using some TLR antagonists in Fig. 1E, mice were injected i.p. with 50 μg polyI:C (GE Bioscience), 50 μg Pam3CSK4 (Boehringer Ingelheim), 10 μg LPS (Sigma-Aldrich), 50 μg R837 (InvivoGen), and 50 μg CpG ODN1826 (InvivoGen). In other experiments, polyI:C was injected i.p. at a dose of 200 μg/mouse.

Cells

For isolation of DC subsets, Mφs and NK cells, spleens were treated with 400 Mandle U/ml collagenase D (Roche) at 37°C for 25 min in HBSS (Sigma-Aldrich). EDTA was added, and the cell suspension was incubated for an additional 5 min at 37°C. NK cells were purified from spleens by positive selection of DX5-positive cells with DX5 MACS beads (Miltenyi Biotec). CD8α$^+$ cDCs were purified using a CD8α$^+$ DC isolation kit and CD11c MACS beads (Miltenyi Biotec). CD8α$^-$ cDCs were purified with CD11c MACS beads (Miltenyi Biotec) from the negative fraction after CD8α$^+$ cDC separation. F4/80$^+$ Mφs were isolated using MACS-positive selection beads (Miltenyi Biotec) as described previously (13). pDC Ag-1$^+$ pDCs were isolated with pDC Ag-1 MACS beads (Miltenyi Biotec). All immune cells were purified from spleens by repeated positive selection to achieve high purity (90%). Leukocytes from the lung were prepared as previously reported (18). Mouse immune cells were cultured in RPMI 1640/10% FCS/55 μM 2-ME/10 mM HEPES. B16D8, B16F10, YAC-1, and RMA-S were cultured in RPMI 1640/10% FCS.

Cell culture

To investigate potential interactions with NK–accessory cells, MACS-sorted accessory cells were cocultured with freshly isolated NK cells (accessory cells /NK = 1:2) with or without 20 μg/ml polyI:C for 24 h. In some coculture experiments using the transwell system, NK cells were added to 0.4-μm pore transwells (Corning) in the presence of polyI:C. Activation of NK cells was assessed by measuring the concentration of IFN-γ (ELISA; GE Healthcare) in the medium. For the IFN (α and β) receptor 1 (IFNAR1) blocking experiment, anti-IFNAR Ab at a final concentration of 10 μg/ml was added to the cultures before addition of polyI:C. For measurement of IL-12p40 and type I IFNs, we used ELISA kits purchased from BioLegend and PBL Biomedical Laboratories, respectively.

FACS analysis

For intracellular cytokine staining of NK cells, we isolated spleen or lung from polyI:C- or PBS-injected mice at each time point and harvested their leukocytes as described previously (18, 19). The leukocytes were incubated in medium with 10 μg/ml brefeldin A for 4 h. Cells were fixed and stained with a combination of anti-NK1.1 (PK136) and anti-CD3ε (145-2C11) Abs (BioLegend), followed by permeabilization and staining with anti-IFN-γ (XMG1.2) Ab (BioLegend), anti–granzyme B (NGZB) Ab (eBioscience), anti–TNF-α (MP6-XT22) Ab (BioLegend), anti–GM-CSF (MP1-22E9) Ab (BioLegend), or anti–IL-2 (JES6-5H4) Ab (BioLegend) using a BD Cytofix/Cytoperm Kit (BD Biosciences). For staining of the C terminus of INAM of each immune cell type, after treatment of anti-CD16/32 (no. 93), cell-surface molecules of splenocytes were stained with anti-CD3ε (145-2C11), anti-CD8α (53-6.7), anti-CD11c (N418), anti-NK1.1, anti-F4/80 (BM8), anti-Gr1 (RB6-8C5), anti-CD11b (M1/70), or anti-CD19 (MB19-1) Abs (BioLegend) or with anti-B220 (RA3-6B2) or anti-CD4 (L3T4) Abs (eBioscience). After staining of the cell surface, cells were fixed and permeabilized using a BD Cytofix/Cytoperm Kit (BD Biosciences) and then stained with an anti-INAM polyclonal Ab as described previously (16). To detect activating markers, NK receptors, and developmental markers, splenocytes were stained with anti-CD27 (LG.3A10), anti-CD25 (PC61), anti-NKp46 (29A1.4), anti-NKG2D (C7), anti-DNAM-1 (10E5), and anti-TRAIL (N2B2) Abs from BioLegend or anti-Fas (Jo2) from BD Biosciences. For detection of dead cells, samples were stained with ViaProbe from BD Biosciences. Samples were processed on an FACSCalibur flow cytometer and analyzed with FlowJo software (Tree Star).

Tumor inoculation and polyI:C treatment

PolyI:C therapy against mice with B16D8 tumor burden was described previously (8). B16F10 melanoma cells (2×10^5) were injected into wild-type (WT) or *Inam*$^{-/-}$ mice via the tail vein on day 0. PolyI:C was injected i.p. on days 1, 4, 7, and 10 at a dose of 200 μg/mouse. The control group was treated with PBS. All mice were killed 12 d after tumor inoculation. The lungs were excised and fixed in Mildform (Wako) for counting of surface colonies under a dissection microscope.

Statistical analysis

Statistical analyses were made with the Student *t* test for paired data. Statistical analyses were made with ANOVA in multiple comparisons. The *p* value of significant differences is reported.

Results

Generation of INAM-deficient mice

We designed a targeting vector to disrupt exon 2, which encodes the C-terminal transmembrane and cytoplasmic regions of INAM

(Fig. 1A). The heterozygosity and homozygosity of siblings were verified by Southern blot analysis (Fig. 1B). Mutant mice were born at the expected Mendelian ratio from *Inam*$^{-/-}$ and *Inam*$^{+/-}$ parents and showed normal healthy development under specific pathogen-free conditions (Fig. 1C). We also examined the composition of immune cells in the spleen and found no clear difference between WT and *Inam*$^{-/-}$ mice (Table I). Murine NK cells are divided into four subsets in their maturation stage based on the surface density of CD27 and CD11b: CD11b^{low}/CD27^{low}, CD11b^{low}/CD27^{high}, CD11b^{high}/CD27^{high}, and CD11b^{high} /CD27^{low} (20). We examined the composition of splenic NK cells in each maturation stage and found no clear difference between WT and *Inam*$^{-/-}$ mice (Supplemental Fig. 1A). A previous study showed that *Inam* mRNA is highly expressed in spleen and thymus under steady-state conditions

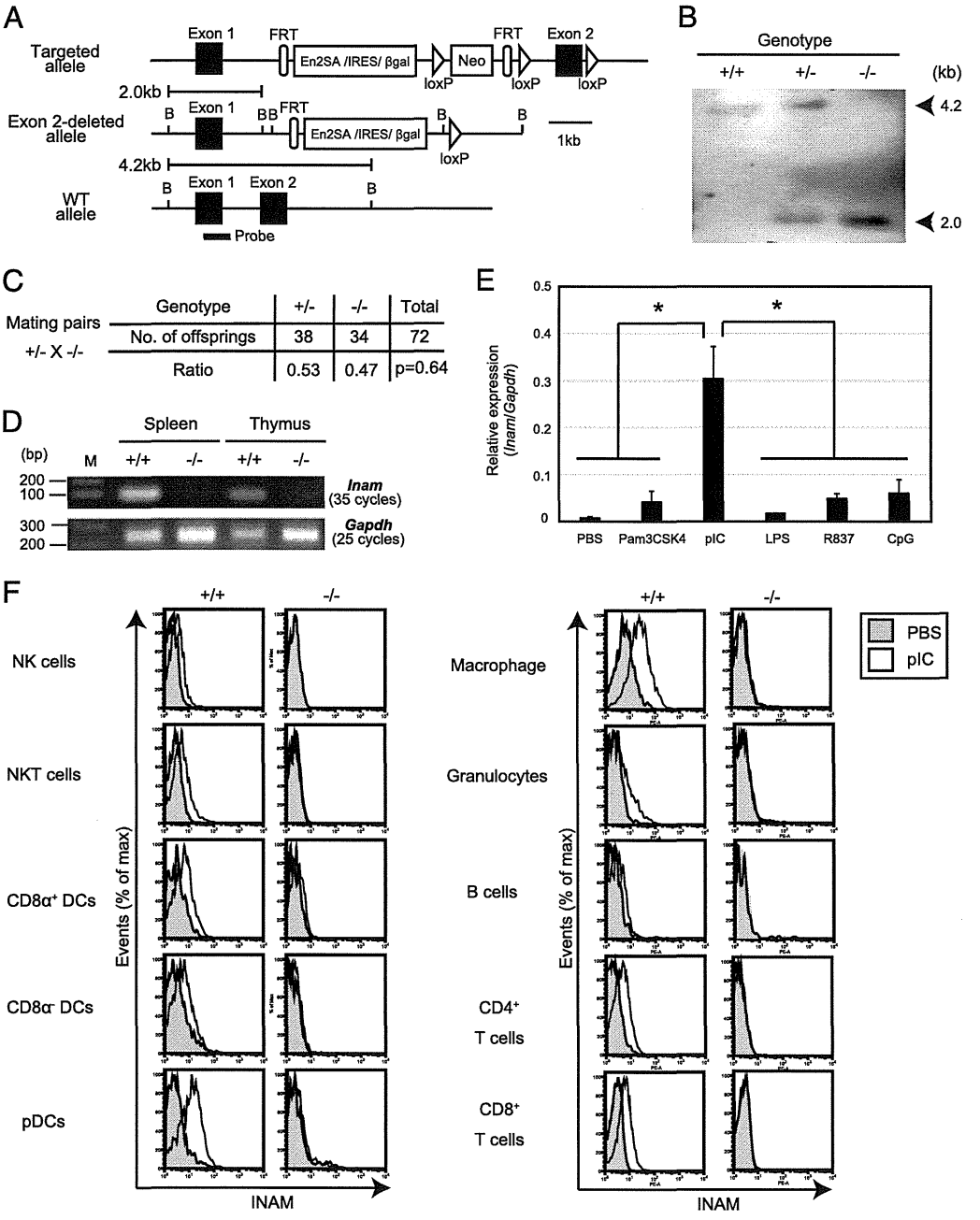

FIGURE 1. Generation of INAM-deficient mice. (**A**) Structure of the mouse *Inam*-targeted, *Inam*-disrupted, and WT allele. Closed boxes indicate the coding exon of Inam. A probe (602 bp) for Southern blot analysis was designed in exon 1. (**B**) Southern blot analysis of BamHI-digested genomic DNA isolated from WT (+/+), heterozygous mutant (+/−), and homozygous mutant (−/−) mice. (**C**) Genotype analyses of offspring from heterozygote intercrosses. The χ^2 goodness-of-fit test indicated that deviation from the Mendelian ratio was not statistically significant ($p > 0.1$). (**D**) RT-PCR analysis of spleen and thymus. Total RNA sets from spleen and thymus in WT (+/+) and *Inam*$^{-/-}$ (−/−) mice were extracted and subjected to RT-PCR to determine *Inam* expression. (**E**) *Inam* mRNA expression in response to TLR agonists. Total RNA were isolated from the spleens of mice in each group ($n = 3$) at 3 h after TLR agonist stimulation and subjected to quantitative PCR to determine to determine *Inam* expression. *$p < 0.05$ (**F**) INAM expression of immune cells. WT (+/+) and *Inam*$^{-/-}$ (−/−) mice were i.p. injected with 200 μg polyI:C (pIC) or PBS ($n = 2$). After 12 h, INAM expression of each immune cell type was analyzed by flow cytometry. Open histograms and shaded histograms indicate immune cells derived from the mice. Immune cells were classified as NK cells (CD3ε$^-$/NK1.1$^+$), NKT cells (CD3ε$^-$/NK1.1^{int}), B cells (CD19c$^+$/B220$^+$), CD8$^+$ T cells (CD3ε$^+$/CD8α$^+$), CD4$^+$ T cells (CD3ε$^+$/CD4α$^+$), classic CD8α$^-$ cDCs (CD11c^{high}/CD8α$^-$), classic CD8α$^+$ cDCs (CD11c^{high}/CD8α$^+$), pDCs (CD11c^{int}/B220$^+$), Mφs (CD11c$^{low\text{-}dim}$/CD11b$^{low\text{-}dim}$/F4/80$^+$), and granulocytes (CD11b^{high}/Gr-1$^+$). The data shown are representative of at least two independent experiments.

Table I. Development of hematopoietic cells in INAM-deficient mice

Cells	WT	*Inam*$^{-/-}$	Student *t* Test
CD4$^+$ T cells	16.9 ± 0.3	16.2 ± 2.2	$p = 0.69$
CD8$^+$ T cells	8.6 ± 0.5	8.0 ± 1.0	$p = 0.27$
B cells	55.6 ± 1.9	56.4 ± 3.5	$p = 0.65$
NK cells	1.2 ± 0.4	2.3 ± 0.7	$p = 0.22$
NKT cells	0.9 ± 0.1	0.76 ± 0.2	$p = 0.27$
pDCs	1.0 ± 0.1	1.0 ± 0.1	$p = 0.91$
CD8α$^+$ DCs	0.2 ± 0.01	0.3 ± 0.02	$p = 0.03$
CD8α$^-$ DCs	0.49 ± 0.03	0.8 ± 0.2	$p = 0.09$
Granulocytes	0.3 ± 0.04	1.0 ± 1.2	$p = 0.43$
Mφ	1.8 ± 0.6	2.2 ± 0.8	$p = 0.45$
Resident monocytes	0.4 ± 0.1	0.4 ± 0.1	$p = 0.96$
Inflammatory monocytes	0.2 ± 0.03	0.2 ± 0.2	$p = 0.82$

Data are percentages unless otherwise indicated.

(16). In our study, mRNA expression of *Inam* in these tissues was clearly absent in the *Inam*-null mouse (Fig. 1D). To assess the induction of *Inam* mRNA expression in response to TLR agonists in vivo, we performed qPCR analysis using spleens at 3 h after i.p. administration of those agonists or PBS. The levels of *Inam* mRNA expression was strongly induced by polyI:C, but not other TLR agonists (Fig. 1E). Hence, these data indicate that polyI:C is the strongest TLR agonist to induce *Inam* expression of the TLR agonists tested in vivo. To investigate the cellular distribution of INAM protein expression, we performed flow cytometric analysis using polyclonal Abs to mouse INAM after i.p. administration of polyI:C. The levels of INAM protein expression in these cells clearly reflected the absence of the mRNA (Fig. 1F). Flow cytometric analysis of spleen cells demonstrated that INAM expression was induced in all myeloid lineage cells, including DC subsets and NK cells. In particular, INAM expression was highly induced in pDCs and F4/80$^+$ Mφs.

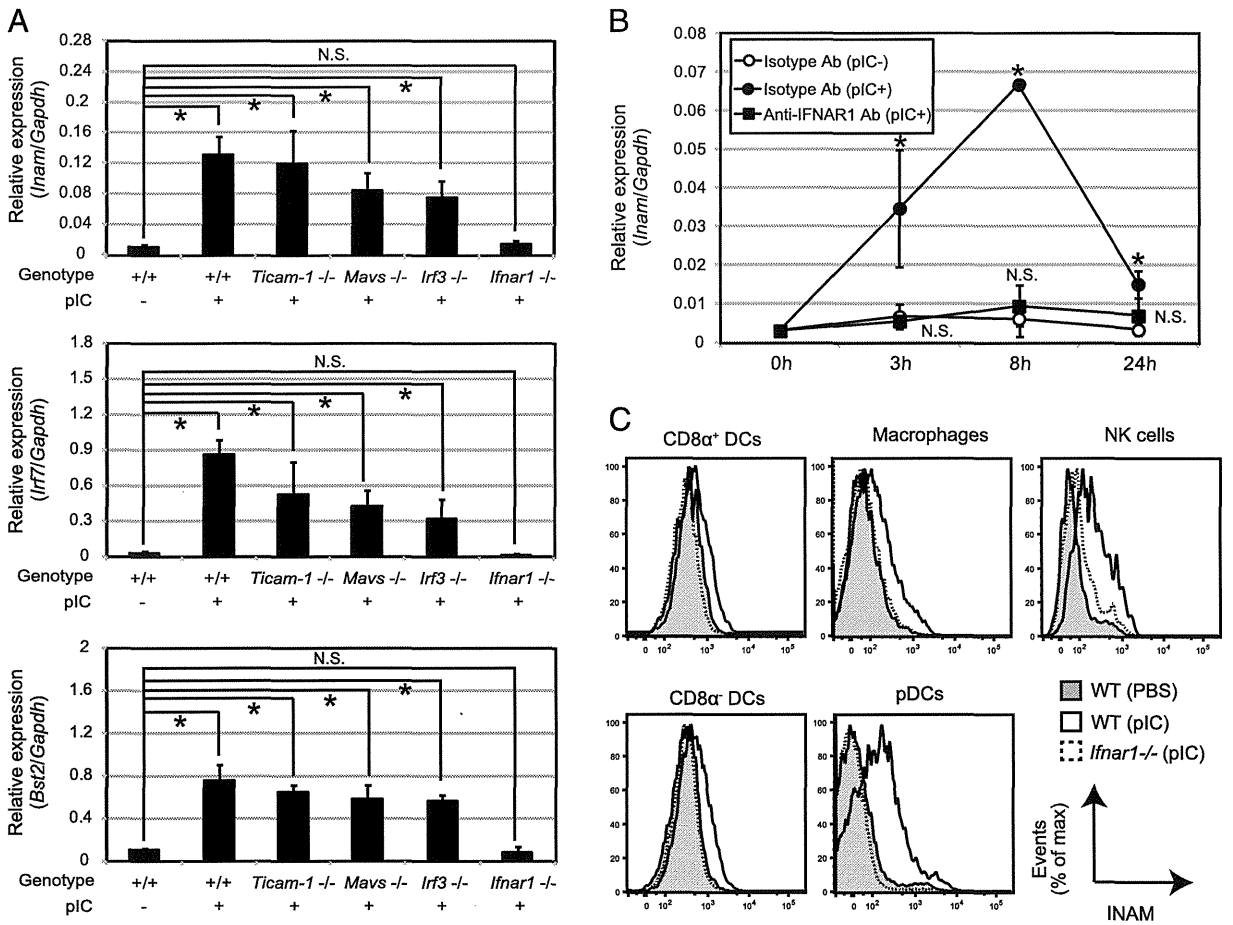

FIGURE 2. Signaling pathway of INAM induction in vivo. (**A**) *Inam* expression in splenocytes derived from various gene-manipulated mice. After 3 h, total RNA were isolated from the spleens of mice in each group ($n = 3$) and subjected to quantitative PCR to determine *Inam*, *Irf7*, and *Bst2* expression. (**B**) Type I IFN signaling is required for *Inam* expression of splenocytes derived from WT mice. Splenocytes ($n = 3$) were treated with polyI:C (pIC), IFNAR1-blocking Ab, or isotype control Ab for 0, 3, 8, and 24 h. (**C**) Type I IFN signaling is required for INAM expression of DC subsets, NK cells, and Mφs. WT and *Ifnar1*$^{-/-}$ mice were i.p. injected with 200 μg polyI:C or PBS ($n = 2$). After 12 h, INAM expression of each immune cell type was analyzed by flow cytometry. The data shown are representative of at least two independent experiments. Data are means ± SD of three independent samples. *$p < 0.05$.

Type I IFN signaling is required for INAM induction in vivo

The TLR3/TICAM-1 and MDA5/mitochondrial antiviral signaling protein pathways activate the transcription factor IRF3 in response to viral RNA. In BMDC, polyI:C (an analog of virus dsRNA) directly induces INAM expression via the TICAM-1/IRF3 pathway (16). Moreover, in the absence of pattern recognition receptor signals, IFN-α stimulation triggers INAM expression in BMDC. However, it is unclear which innate signal is required for its up-regulation in vivo. To understand the inducible pathway of *Inam* expression, we investigated its expression in spleen cells derived from various genetically manipulated mice. After polyI:C stimulation, *Inam* expression was completely undetectable in IFN (α and β) receptor 1 $(Ifnar1)^{-/-}$ mice, but not in $Ticam\text{-}1^{-/-}$ mice, a similar pattern of expression to that seen in type I IFN–inducible genes including *Irf7* and *Bst2* (Fig. 2A). Additionally, *Inam* expression was partially reduced in mice deficient in *Mavs* or *Irf3*, factors that are critical for producing type I IFN in response to polyI:C (3, 16). To assess the effect of type I IFN in WT mice, splenocytes were stimulated with polyI:C in the presence of anti-IFNAR1 Ab or isotype control Ab. Expression of *Inam* was transient, peaking at 8 h in the stimulated group in the presence of isotype control Ab (Fig. 2B). In contrast, blocking of the type I IFN receptor led to abrogation of *Inam* induction. In agreement with these results, INAM protein expression was completely undetectable in DC subsets, NK cells, and Mφs derived from IFNAR1-deficient mice (Fig. 2C). Hence, these data indicate that INAM expression depends on the IFNAR1 signaling pathway in vivo.

INAM is required for IFN-γ production through NK–accessory interaction

To identify the accessory cells directly responding to polyI:C and leading to IFN-γ production from NK cells, we performed an experiment on a coculture consisting of MACS-sorted splenic NK cells and myeloid immune cells including DC subsets and Mφs. Purified NK cells cultured in medium with or without polyI:C did not produce IFN-γ (Fig. 3A). In contrast, a high level of IFN-γ production was observed in the supernatant of NK cells cocultured with $CD8\alpha^+$ cDCs and Mφs in the presence of polyI:C, but not in pDCs and $CD8\alpha^-$ cDCs. In our reports, cell-to-cell contact is required for the interaction between NK cells and BMDC (8, 16). To confirm that the cell-to-cell contact is a prerequisite for the interaction between NK cells and splenic accessory cells, we performed coculture experiments using transwell system. As

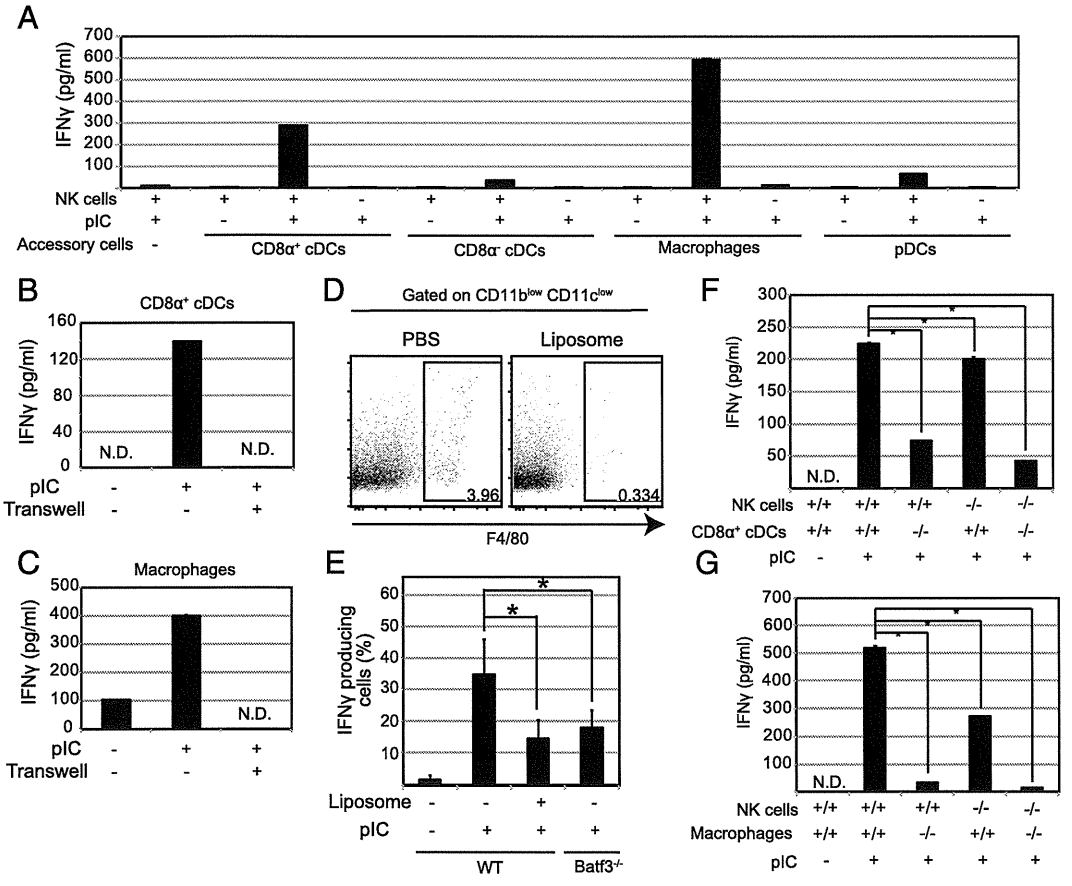

FIGURE 3. INAM-dependent NK cell activation in vitro. (**A**) IFN-γ production of NK cells via polyI:C (pIC)-stimulated DC subsets and Mφs. NK cells, DC subsets, and Mφs were enriched by MACS separation from WT and $Inam^{-/-}$ mice. (**B**) Cell-to-cell contact-dependent NK cell activation via $CD8\alpha^+$ cDCs. (**C**) Cell-to-cell contact-dependent NK cell activation via Mφs. NK cells were cocultured with DC subsets and Mφs in the presence of polyI:C (20 μg/ml) for 24 h. The concentrations of IFN-γ in the culture supernatants were measured by ELISA. (**D**) Mφ depletion with clodronate liposomes. WT mice were i.p. injected with clodronate liposomes (150 μl/mouse) to remove Mφs. After 24 h, the efficiency of Mφ depletion was measured by FACS analysis. (**E**) Production of IFN-γ by NK cells in WT, Mφ-depleted WT, and $Batf3^{-/-}$ mice. WT, Mφ-depleted WT, and $Batf3^{-/-}$ mice were i.p. injected with 200 μg polyI:C ($n = 3$). After 3 h, splenocytes were isolated, cultured with brefeldin A for an additional 4 h, and analyzed for intracellular content of IFN-γ by FACS, gating on $CD3\varepsilon^-$/$NK1.1^+$ cells. (**F**) INAM-dependent NK cell activation via $CD8\alpha^+$ cDCs. (**G**) INAM-dependent NK cell activation via Mφs. NK cells, $CD8\alpha^+$ cDCs, and Mφs were enriched via MACS separation from WT and $Inam^{-/-}$ mice. NK cells were cocultured with $CD8\alpha^+$ cDCs or Mφs in the presence of polyI:C (20 μg/ml) for 24 h. The concentrations of IFN-γ in the culture supernatants were measured by ELISA. The data shown are representative of at least two independent experiments. Data are means ± SD of three independent samples. $^*p < 0.05$.

a result, IFN-γ production was completely blocked under transwell conditions (Fig. 3B, 3C). Therefore, NK cells are primed through contact with CD8α$^+$ cDCs and Mφs independent of soluble mediators. To directly test the contribution of CD8α$^+$ cDCs and Mφs to polyI:C-mediated NK cell activation in vivo, we analyzed *Batf3*$^{-/-}$ mice, which largely lack the CD8α$^+$ cDC population in the spleen of C57BL/6 mice (21), and Mφ-depleted mice generated by clodronate liposome injection (22, 23). Approximately 85% of Mφs were depleted at 24 h after clodronate liposome injection (Fig. 3D). Three hours after polyI:C stimulation, NK cell secretion of IFN-γ was partially decreased in *Batf3*$^{-/-}$ and Mφ-depleted mice (Fig. 3E). These results indicate that CD8α$^+$ cDCs and Mφs are responsible for secretion of IFN-γ from NK cells in response to polyI:C stimulation.

INAM acts on NK cells and BMDC to orchestrate NK–DC interaction triggered by polyI:C stimulation (16). To investigate the role of INAM in the interaction of NK-CD8α$^+$ cDC and NK-Mφ, we performed an experiment on a coculture of MACS-sorted splenic NK cells with their accessory cells isolated from WT and *Inam*$^{-/-}$ mice. Cocultures of NK cells and accessory cells lacking INAM showed that IFN-γ production from NK cells required INAM expression in either NK cells or accessory cells (Fig. 3F, 3G). Notably, deficiency of INAM in both NK and accessory cells led to a marked decrease in IFN-γ production. Taken together, these results suggest that INAM is required for cell–cell contact in both NK cells and accessory cells and early IFN-γ production by NK cells.

INAM plays a critical role in rapid IFN-γ production by NK cells in response to polyI:C in vivo

To investigate the role of INAM in polyI:C-mediated cytotoxicity of NK cells, we injected WT and *Inam*$^{-/-}$ mice with polyI:C. After 0, 3, and 24 h, we isolated splenic NK cells and measured cytotoxicity ex vivo. In the four NK-sensitive cell lines B16D8, RMA-S, B16F10, and YAC-1, we found no difference between WT and *Inam*$^{-/-}$ mice in the cytotoxic effect of NK cells against these cell lines (data not shown). Consistent with these results, cell numbers expressing granzyme B, known as a cytotoxic lymphocyte protease, barely differed between splenocytes of WT and *Inam*$^{-/-}$ mice (Fig. 4A). To determine the role of INAM in NK cell production of IFN-γ in response to polyI:C, we isolated splenocytes 0, 1, and 3 h after injecting WT and *Inam*$^{-/-}$ mice with polyI:C and determined the intracellular content of IFN-γ in NK cells. After 3 h, NK cells isolated from *Inam*$^{-/-}$ mice produced less IFN-γ than WT NK cells (Fig. 4B). Additionally, we also measured the numbers of other cytokine-producing cells, including GM-CSF, IL-2, and TNF-α, from NK cells at 3 h after polyI:C stimulation in WT and *Inam*$^{-/-}$ mice and confirmed no INAM dependence of the production of these cytokines (Supplemental Fig. 2A). Therefore, INAM specifically regulates IFN-γ through CD8α DC at least within this time frame. We also measured CD69 expression, known as an NK-activating marker at 0, 3, and 24 h after polyI:C stimulation. CD69 upregulation in response to polyI:C was partially impaired in NK cells from *Inam*$^{-/-}$ mice in comparison with those from WT mice 24 h after polyI:C stimulation (Fig. 4C). We found no clear difference between WT and *Inam*$^{-/-}$ mice in expression of CD27 or NK1.1, both of which evoke IFN-γ production through their interaction with the ligands, or in any other NK receptors at 0, 3, and 24 h after polyI:C injection (24) (Supplemental Fig. 1B). These results indicate that INAM-mediated NK activation is independent of incremental expression of these receptors. Previous reports suggested that proinflammatory cytokines including IL-12, IL-15, IL-18, and type I IFN play critical roles in the cytotoxicity and IFN-γ production of NK cells (15, 25, 26). To determine their expression at 0, 3, and 24 h

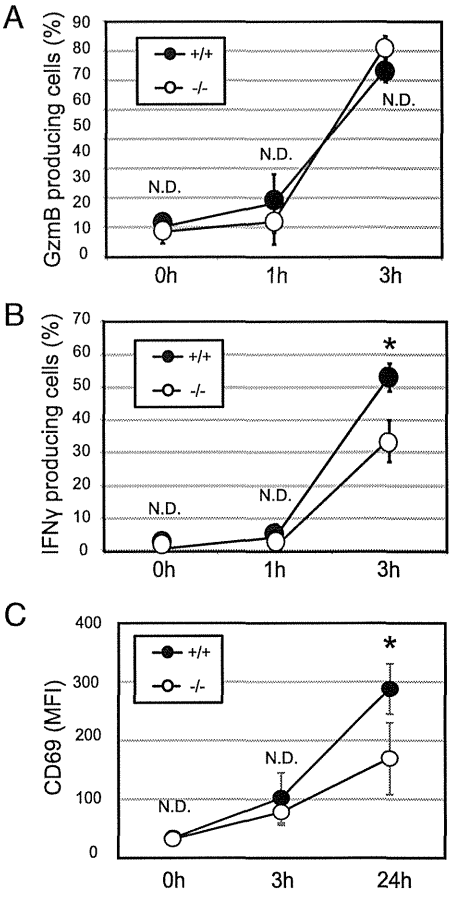

FIGURE 4. INAM-dependent NK cell activation in vivo. (**A**) Production of granzyme B (GzmB) by NK cells. (**B**) Production of IFN-γ by NK cells. WT (+/+) and *Inam*$^{-/-}$ (−/−) mice were i.p. injected with 200 μg polyI:C. After 0, 1, and 3 h, splenocytes were isolated, cultured with brefeldin A for an additional 4 h, and analyzed for intracellular content of IFN-γ and granzyme B by FACS, gating on CD3ε$^-$/NK1.1$^+$ cells (n = 3 or 4). (**C**) Expression of CD69 on the surface of NK cells. WT (+/+) and *Inam*$^{-/-}$ (−/−) mice were i.p. injected with 200 μg polyI:C or PBS. After 0, 3, and 24 h, CD69 expression was assayed by FACS, and the data were quantitatively analyzed using mean fluorescence intensity (MFI), gating on CD3ε$^-$/NK1.1$^+$ cells (n = 3). The data shown are representative of at least two independent experiments. Data are means ± SD of three independent samples. *$p < 0.05$.

after polyI:C stimulation, we performed ELISA and qPCR analysis of serum and spleen cells from WT and *Inam*$^{-/-}$ mice. However, protein levels of IL12p40, IFN-α, and IFN-β were not affected by *Inam* disruption in mice (Supplemental Fig. 2B). Additionally, mRNA expression of *Il-15* and *Il-18* genes was not decreased in *Inam*$^{-/-}$ mice (Supplemental Fig. 2C). These results suggest that INAM plays a critical role in the CD69 expression and rapid IFN-γ production, but not the cytotoxicity, of NK cells in response to polyI:C in a cytokine-independent manner.

INAM is required for the antimetastatic effect by polyI:C-based cancer immunotherapy

Malignant melanomas are one of the most important targets of NK-mediated cancer immunotherapy (27). In this study, we tested two types of polyI:C-based cancer immunotherapy model using B16D8 and B16F10 cell lines. NK cells show high cytotoxicity activity against B16D8 cells established in our laboratory as a subline of the B16 melanoma cell line (28). This subline was characterized by its low or virtually absent metastatic properties when injected s.c. into syngeneic C57BL/6 mice. In contrast, the B16F10 subline was characterized by its high metastatic capacity

especially into the lung (29). In this model, NK1.1$^+$ cells and IFN-γ have a critical role in the suppression of pulmonary metastases (30).

A mouse model with s.c.-implanted B16D8 and polyI:C therapy has been established in our laboratory (8). To investigate the function of INAM involved in tumor growth retardation mediated by polyI:C, we challenged WT and *Inam*$^{-/-}$ mice with B16D8 implantation and then treated the mice with i.p. injection of polyI:C. The rate of B16D8 growth retardation was indistinguishable between WT and *Inam*$^{-/-}$ mice (Supplemental Fig. 3), which was largely dependent on the antitumor effect of polyI:C. This result is consistent with the observation that there is no difference in tumoricidal activity against B16D8 between WT and *Inam*$^{-/-}$ mice. To determine the role of INAM in the production of IFN-γ by lung NK cells in response to polyI:C, we isolated leukocytes from the lung at 0, 3, and 6 h after administration of polyI:C to B16F10-injected WT and *Inam*$^{-/-}$ mice and determined the intracellular content of IFN-γ in NK cells (Fig. 5A). After 6 h, NK cells isolated from *Inam*$^{-/-}$ mice produced less IFN-γ than WT NK cells (Fig. 5B). To investigate the function of INAM involved in pulmonary metastases induced by polyI:C, we i.v. challenged WT and *Inam*$^{-/-}$ mice with B16F10 cells and then treated the mice by i.p. injection of polyI:C. After four rounds of polyI:C treatment, we counted tumor foci in the lung. Under unstimulated conditions, there was no difference in the number and size of tumor foci in the lungs between WT and *Inam*$^{-/-}$ mice (Fig. 5C). In WT mice, i.p. injection of polyI:C exerted a significant inhibition in the growth of pulmonary metastases in tumor-bearing mice compared with PBS controls (Fig. 5D). In contrast, the effect of polyI:C therapy for pulmonary metastases was partially abrogated in *Inam*$^{-/-}$ mice. These results demonstrate that INAM plays a critical role in IFN-γ production by lung NK cells in response to polyI:C and unequivocally exhibits antitumor function in polyI:C-based cancer immunotherapy against IFN-γ–sensitive tumors metastasized to the lung.

BMDC confer direct cytotoxic activity on NK cells by stimulation with RNA via INAM-dependent cell–cell contact (16). Then, NK cells kill tumor cells via effectors, such as TRAIL and granzyme B, secondary to upregulation of INAM. However, splenic DCs hardly induce direct NK cytotoxicity as shown in this study. In this study, *Inam*$^{-/-}$ mice studies revealed that DC/Mφ primed NK cells in vivo to induce IFN-γ that was a major effector for NK antimetastatic activity. Thus, taken together with the previous results that BMDCs induce NK cytotoxicity via INAM (16), INAM-involved DC–NK contact induces two arrays of NK tumoricidal activities, killer effector and IFN-γ producer, depending on the properties of DC subsets. The role of INAM in ILC activation will be a matter of future interest in this context.

Discussion

In this study, we provide the first demonstration, to our knowledge, that INAM plays a critical role in the interactions of NK-CD8α$^+$ cDCs and Mφs leading to IFN-γ production from NK cells in vivo. Additionally, we also propose that INAM is a novel target molecule for cancer immunotherapy against IFN-γ–suppressible metastasis.

IFN-γ coordinates a diverse array of cellular programs via STAT1 activation, such as antimicrobial response, anti- or protumor response, production of proinflammatory cytokines, and induction of IRF1 (31). IRF1 activates a large number of secondary response genes, which carry out a range of immunomodulatory functions (32, 33). In secondary lymphoid organs including spleen and lymph nodes, NK cells are a dominant IFN-γ producer responding to polyI:C (5). IFN-γ primes Ag-specific CD4$^+$ and CD8$^+$ T cells and also activates other innate immune cells including Mφs (34–36). The TLR3-dependent IFN-γ signaling pathway is important in protecting the host from pathogenesis induced by Coxsackievirus group B serotype 3 infection, which leads to IFN-γ production from NK cells (37, 38). Hence, IFN-γ

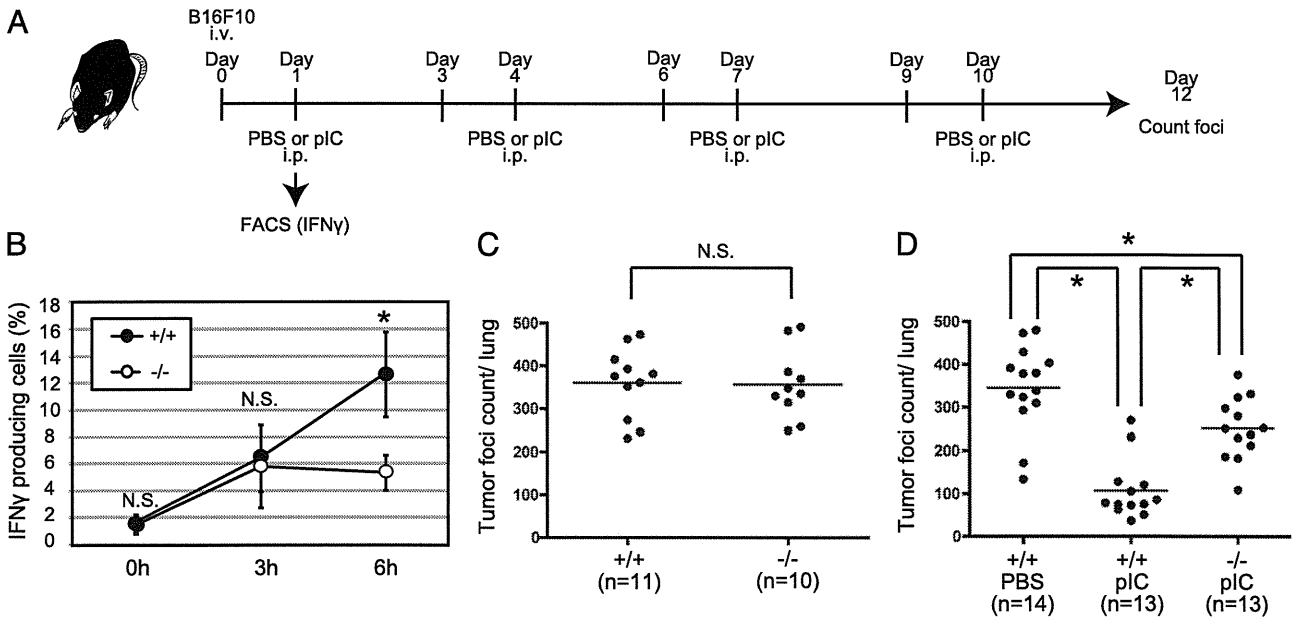

FIGURE 5. Antimetastatic activity of INAM against B16F10 melanoma. (**A**) The time schedule of polyI:C (pIC) treatment. (**B**) Production of IFN-γ by NK cells in the lung. After 24 h, WT and *Inam*$^{-/-}$ mice were i.p. injected with 200 μg polyI:C. Lung leukocytes were isolated and cultured with brefeldin A for an additional 4 h, and analyzed for frequency of NK cells and production of IFN-γ/granzyme B by FACS, gating on CD3ε$^-$/NK1.1$^+$ cells ($n = 3$ or 4). (**C**) Tumor foci counts in the lung of WT (+/+) and *Inam*$^{-/-}$ (−/−) mice under unstimulated conditions at day 12. (**D**) Tumor foci in the lung of WT (+/+) and *Inam*$^{-/-}$ (−/−) mice. WT (+/+) and *Inam*$^{-/-}$ (−/−) mice were i.v. injected with 2×10^5 B16F10 melanoma cells at day 0. At days 1, 4, 7, and 10, WT and *Inam*$^{-/-}$ mice were i.p. injected with 200 μg polyI:C. At day 12, the mice were sacrificed, and lungs were removed and fixed in 10% formalin solution to count surface colonies under a dissection microscope. The data shown are representative of at least two independent experiments. Data are means ± SD of three independent samples. *$p < 0.05$.

derived from NK cells controls innate and adaptive immunity, leading to a Th1 response.

In this study, we show that INAM evokes IFN-γ production by NK cells in the early phase by polyI:C stimulation (Figs. 4B, 5B). In a murine CMV infection model, IFN-γ is induced in NK cells by IL-12 and IL-18 produced by murine CMV–infected CD11b$^+$ cDCs, whereas these cytokines barely evoke any cytotoxic response in NK cells (39). In addition, IFN-γ production from NK cells is induced by anti-CD27 Ab stimulation, but again no cytotoxic response is triggered (24). Therefore, these reports indicate that NK cell cytotoxicity and IFN-γ production are independently controlled by different mechanisms. We found no clear difference between WT and *Inam*$^{-/-}$ mice in expression of these cell surface molecules and cytokines. Hence, the INAM-dependent IFN-γ production from NK cells is based on an as-yet-unknown mechanism(s) acting in a manner independent of these molecules.

CpG DNA is known to induce IFN-γ from NK cells, which is mediated through pDCs. TLR9 in pDCs responds to CpG, and the pDCs liberate IFN-α and TNF-α that participate in the induction of IFN-γ from NK cells (40). We checked induction of the Inam mRNA in spleen after stimulation with CpG in WT and *Inam*$^{-/-}$ mice (Fig. 1E). The levels of *Inam* mRNA as well as numbers of IFN-γ–producing cells were hardly increased in response to i.p. administration of CpG in WT as well as *Inam*$^{-/-}$ mice, suggesting no participation of INAM in CpG-induced NK cell IFN-γ production (data not shown). CpG participates in the activation of the TLR9 pathway in pDCs, but INAM in splenic cDCs and Mφs does not participate in CpG-mediated NK priming. The result is consistent with the fact that polyI:C is an agonist for TLR3 (but not for TLR9 predominantly expressed in pDCs), which is mainly expressed in CD8α$^+$ DCs, especially professional Ag-presenting CD141$^+$ and CD103$^+$ DCs in mice (41).

CD8α$^+$ cDCs directly recognize polyI:C via the TLR3/TICAM-1 pathway and promote IFN-γ production from NK cells in vitro (9). However, previous analysis of *Batf3*$^{-/-}$ mice indicated that absence of CD8α$^+$ cDCs resulted in weak NK cell activation, in agreement with our data (19). We also found that NK cell secretion of IFN-γ was partially decreased in mice depleted of Mφs by injection of clodronate liposomes (Fig. 3E). Notably, expression of INAM by both NK cells and accessory cells is required for early IFN-γ production through NK-CD8α$^+$ cDC and/or NK–Mφ interactions (Fig. 3F, 3G). The physiological role of these accessory cells in NK activation is poorly understood. However, our results indicate that CD8α$^+$ cDCs and Mφs facilitate early secretion of IFN-γ from NK cells in response to polyI:C and INAM plays a critical role in the interaction between NK cells and CD8α$^+$ cDCs and/or Mφs, leading to IFN-γ production.

IFN-γ exhibits both anti- and protumor activities (42). Systemic administration of polyI:C exerted a significant inhibitory effect on the growth of lung metastases in B16F10 melanoma-bearing mice (30, 42). Using this model, a previous study reported that NK1.1$^+$ cells and IFN-γ have a critical role in the protection of lung metastases (30). Previous studies demonstrated that the IFN-γ receptor expressed on host cells, but not on melanoma cells, is important for development of lung metastases (43–45). Hence, lung metastases are prevented by the IFN-γ–inducible immune response following NK cell activation. We show that INAM is involved in the IFN-γ production of lung NK cells in response to polyI:C stimulation and unequivocally exhibits antitumor functions in polyI:C-based cancer immunotherapy against IFN-γ–sensitive tumor foci in the lung (Fig. 5D). Therefore, we propose that INAM is a novel target molecule for cancer immunotherapy against IFN-γ–suppressible metastasis.

Acknowledgments

We thank the members in Seya Laboratory (Hokkaido University). Tumor implant studies were supported by A. Morii-Sakai (Seya Laboratory). Thoughtful discussions with Dr. T. Taniguchi (University of Tokyo) are gratefully acknowledged.

Disclosures

The authors have no financial conflicts of interest.

References

1. Seya, T., J. Kasamatsu, M. Azuma, H. Shime, and M. Matsumoto. 2011. Natural killer cell activation secondary to innate pattern sensing. *J. Innate Immun.* 3: 264–273.
2. Reed, S. G., M. T. Orr, and C. B. Fox. 2013. Key roles of adjuvants in modern vaccines. *Nat. Med.* 19: 1597–1608.
3. Kumar, H., S. Koyama, K. J. Ishii, T. Kawai, and S. Akira. 2008. Cutting edge: cooperation of IPS-1- and TRIF-dependent pathways in poly IC-enhanced antibody production and cytotoxic T cell responses. *J. Immunol.* 180: 683–687.
4. Trumpfheller, C., M. Caskey, G. Nchinda, M. P. Longhi, O. Mizenina, Y. Huang, S. J. Schlesinger, M. Colonna, and R. M. Steinman. 2008. The microbial mimic poly IC induces durable and protective CD4$^+$ T cell immunity together with a dendritic cell targeted vaccine. *Proc. Natl. Acad. Sci. USA* 105: 2574–2579.
5. Longhi, M. P., C. Trumpfheller, J. Idoyaga, M. Caskey, I. Matos, C. Kluger, A. M. Salazar, M. Colonna, and R. M. Steinman. 2009. Dendritic cells require a systemic type I interferon response to mature and induce CD4+ Th1 immunity with poly IC as adjuvant. *J. Exp. Med.* 206: 1589–1602.
6. Talmadge, J. E., J. Adams, H. Phillips, M. Collins, B. Lenz, M. Schneider, E. Schlick, R. Ruffmann, R. H. Wiltrout, and M. A. Chirigos. 1985. Immunomodulatory effects in mice of polyinosinic-polycytidylic acid complexed with poly-L-lysine and carboxymethylcellulose. *Cancer Res.* 45: 1058–1065.
7. Spits, H., D. Artis, M. Colonna, A. Diefenbach, J. P. Di Santo, G. Eberl, S. Koyasu, R. M. Locksley, A. N. McKenzie, R. E. Mebius, et al. 2013. Innate lymphoid cells—a proposal for uniform nomenclature. *Nat. Rev. Immunol.* 13: 145–149.
8. Akazawa, T., T. Ebihara, M. Okuno, Y. Okuda, M. Shingai, K. Tsujimura, T. Takahashi, M. Ikawa, M. Okabe, N. Inoue, et al. 2007. Antitumor NK activation induced by the Toll-like receptor 3-TICAM-1 (TRIF) pathway in myeloid dendritic cells. *Proc. Natl. Acad. Sci. USA* 104: 252–257.
9. Miyake, T., Y. Kumagai, H. Kato, Z. Guo, K. Matsushita, T. Satoh, T. Kawagoe, H. Kumar, M. H. Jang, T. Kawai, et al. 2009. Poly I:C-induced activation of NK cells by CD8 alpha+ dendritic cells via the IPS-1 and TRIF-dependent pathways. *J. Immunol.* 183: 2522–2528.
10. Wulff, S., R. Pries, and B. Wollenberg. 2010. Cytokine release of human NK cells solely triggered with Poly I:C. *Cell. Immunol.* 263: 135–137.
11. Fuchs, A., W. Vermi, J. S. Lee, S. Lonardi, S. Gilfillan, R. D. Newberry, M. Cella, and M. Colonna. 2013. Intraepithelial type 1 innate lymphoid cells are a unique subset of IL-12- and IL-15-responsive IFN-γ-producing cells. *Immunity* 38: 769–781.
12. Matsumoto, M., K. Funami, H. Oshiumi, and T. Seya. 2013. Toll-IL-1-receptor-containing adaptor molecule-1: a signaling adaptor linking innate immunity to adaptive immunity. *Prog. Mol. Biol. Transl. Sci.* 117: 487–510.
13. Shime, H., A. Kojima, A. Maruyama, Y. Saito, H. Oshiumi, M. Matsumoto, and T. Seya. 2014. Myeloid-derived suppressor cells confer tumor-suppressive functions on natural killer cells via polyinosinic:polycytidylic acid treatment in mouse tumor models. *J. Innate Immun.* 6: 293–305.
14. Tu, Z., A. Bozorgzadeh, R. H. Pierce, J. Kurtis, I. N. Crispe, and M. S. Orloff. 2008. TLR-dependent cross talk between human Kupffer cells and NK cells. *J. Exp. Med.* 205: 233–244.
15. Lucas, M., W. Schachterle, K. Oberle, P. Aichele, and A. Diefenbach. 2007. Dendritic cells prime natural killer cells by trans-presenting interleukin 15. *Immunity* 26: 503–517.
16. Ebihara, T., M. Azuma, H. Oshiumi, J. Kasamatsu, K. Iwabuchi, K. Matsumoto, H. Saito, T. Taniguchi, M. Matsumoto, and T. Seya. 2010. Identification of a polyI:C-inducible membrane protein that participates in dendritic cell-mediated natural killer cell activation. *J. Exp. Med.* 207: 2675–2687.
17. Sato, M., H. Suemori, N. Hata, M. Asagiri, K. Ogasawara, K. Nakao, T. Nakaya, M. Katsuki, S. Noguchi, N. Tanaka, and T. Taniguchi. 2000. Distinct and essential roles of transcription factors IRF-3 and IRF-7 in response to viruses for IFN-alpha/beta gene induction. *Immunity* 13: 539–548.
18. Takaki, H., M. Takeda, M. Tahara, M. Shingai, H. Oshiumi, M. Matsumoto, and T. Seya. 2013. The MyD88 pathway in plasmacytoid and CD4+ dendritic cells primarily triggers type I IFN production against measles virus in a mouse infection model. *J. Immunol.* 191: 4740–4747.
19. McCartney, S., W. Vermi, S. Gilfillan, M. Cella, T. L. Murphy, R. D. Schreiber, K. M. Murphy, and M. Colonna. 2009. Distinct and complementary functions of MDA5 and TLR3 in poly(I:C)-mediated activation of mouse NK cells. *J. Exp. Med.* 206: 2967–2976.
20. Hayakawa, Y., N. D. Huntington, S. L. Nutt, and M. J. Smyth. 2006. Functional subsets of mouse natural killer cells. *Immunol. Rev.* 214: 47–55.
21. Edelson, B. T., T. R. Bradstreet, W. Kc, K. Hildner, J. W. Herzog, J. Sim, J. H. Russell, T. L. Murphy, E. R. Unanue, and K. M. Murphy. 2011. Batf3-dependent CD11b(low/-) peripheral dendritic cells are GM-CSF-independent

and are not required for Th cell priming after subcutaneous immunization. *PLoS ONE* 6: e25660.
22. Hildner, K., B. T. Edelson, W. E. Purtha, M. Diamond, H. Matsushita, M. Kohyama, B. Calderon, B. U. Schraml, E. R. Unanue, M. S. Diamond, et al. 2008. Batf3 deficiency reveals a critical role for CD8alpha$^+$ dendritic cells in cytotoxic T cell immunity. *Science* 322: 1097–1100.
23. Tussiwand, R., W. L. Lee, T. L. Murphy, M. Mashayekhi, W. Kc, J. C. Albring, A. T. Satpathy, J. A. Rotondo, B. T. Edelson, N. M. Kretzer, et al. 2012. Compensatory dendritic cell development mediated by BATF-IRF interactions. *Nature* 490: 502–507.
24. Takeda, K., H. Oshima, Y. Hayakawa, H. Akiba, M. Atsuta, T. Kobata, K. Kobayashi, M. Ito, H. Yagita, and K. Okumura. 2000. CD27-mediated activation of murine NK cells. *J. Immunol.* 164: 1741–1745.
25. Ferlazzo, G., M. Pack, D. Thomas, C. Paludan, D. Schmid, T. Strowig, G. Bougras, W. A. Muller, L. Moretta, and C. Münz. 2004. Distinct roles of IL-12 and IL-15 in human natural killer cell activation by dendritic cells from secondary lymphoid organs. *Proc. Natl. Acad. Sci. USA* 101: 16606–16611.
26. Takeda, K., H. Tsutsui, T. Yoshimoto, O. Adachi, N. Yoshida, T. Kishimoto, H. Okamura, K. Nakanishi, and S. Akira. 1998. Defective NK cell activity and Th1 response in IL-18-deficient mice. *Immunity* 8: 383–390.
27. Burke, S., T. Lakshmikanth, F. Colucci, and E. Carbone. 2010. New views on natural killer cell-based immunotherapy for melanoma treatment. *Trends Immunol.* 31: 339–345.
28. Tanaka, H., Y. Mori, H. Ishii, and H. Akedo. 1988. Enhancement of metastatic capacity of fibroblast-tumor cell interaction in mice. *Cancer Res.* 48: 1456–1459.
29. Brown, L. M., D. R. Welch, and S. R. Rannels. 2002. B16F10 melanoma cell colonization of mouse lung is enhanced by partial pneumonectomy. *Clin. Exp. Metastasis* 19: 369–376.
30. Jiang, Q., H. Wei, and Z. Tian. 2008. IFN-producing killer dendritic cells contribute to the inhibitory effect of poly I:C on the progression of murine melanoma. *J. Immunother.* 31: 555–562.
31. Schroder, K., P. J. Hertzog, T. Ravasi, and D. A. Hume. 2004. Interferon-gamma: an overview of signals, mechanisms and functions. *J. Leukoc. Biol.* 75: 163–189.
32. Honda, K., and T. Taniguchi. 2006. IRFs: master regulators of signalling by Toll-like receptors and cytosolic pattern-recognition receptors. *Nat. Rev. Immunol.* 6: 644–658.
33. Miyamoto, M., T. Fujita, Y. Kimura, M. Maruyama, H. Harada, Y. Sudo, T. Miyata, and T. Taniguchi. 1988. Regulated expression of a gene encoding a nuclear factor, IRF-1, that specifically binds to IFN-beta gene regulatory elements. *Cell* 54: 903–913.
34. O'Sullivan, T., R. Saddawi-Konefka, W. Vermi, C. M. Koebel, C. Arthur, J. M. White, R. Uppaluri, D. M. Andrews, S. F. Ngiow, M. W. L. Teng, et al. 2012. Cancer immunoediting by the innate immune system in the absence of adaptive immunity. *J. Exp. Med.* 209: 1869–1882.
35. Mailliard, R. B., Y. I. Son, R. Redlinger, P. T. Coates, A. Giermasz, P. A. Morel, W. J. Storkus, and P. Kalinski. 2003. Dendritic cells mediate NK cell help for Th1 and CTL responses: two-signal requirement for the induction of NK cell helper function. *J. Immunol.* 171: 2366–2373.
36. Martín-Fontecha, A., L. L. Thomsen, S. Brett, C. Gerard, M. Lipp, A. Lanzavecchia, and F. Sallusto. 2004. Induced recruitment of NK cells to lymph nodes provides IFN-gamma for T(H)1 priming. *Nat. Immunol.* 5: 1260–1265.
37. Hühn, M. H., M. Hultcrantz, K. Lind, H. G. Ljunggren, K. J. Malmberg, and M. Flodström-Tullberg. 2008. IFN-gamma production dominates the early human natural killer cell response to Coxsackievirus infection. *Cell. Microbiol.* 10: 426–436.
38. Negishi, H., T. Osawa, K. Ogami, X. Ouyang, S. Sakaguchi, R. Koshiba, H. Yanai, Y. Seko, H. Shitara, K. Bishop, et al. 2008. A critical link between Toll-like receptor 3 and type II interferon signaling pathways in antiviral innate immunity. *Proc. Natl. Acad. Sci. USA* 105: 20446–20451.
39. Andoniou, C. E., S. L. H. van Dommelen, V. Voigt, D. M. Andrews, G. Brizard, C. Asselin-Paturel, T. Delale, K. J. Stacey, G. Trinchieri, and M. A. Degli-Esposti. 2005. Interaction between conventional dendritic cells and natural killer cells is integral to the activation of effective antiviral immunity. *Nat. Immunol.* 6: 1011–1019.
40. Marshall, J. D., D. S. Heeke, C. Abbate, P. Yee, and G. Van Nest. 2006. Induction of interferon-gamma from natural killer cells by immunostimulatory CpG DNA is mediated through plasmacytoid-dendritic-cell-produced interferon-alpha and tumour necrosis factor-alpha. *Immunology* 117: 38–46.
41. Jongbloed, S. L., A. J. Kassianos, K. J. McDonald, G. J. Clark, X. Ju, C. E. Angel, C. J. Chen, P. R. Dunbar, R. B. Wadley, V. Jeet, et al. 2010. Human CD141+ (BDCA-3)+ dendritic cells (DCs) represent a unique myeloid DC subset that cross-presents necrotic cell antigens. *J. Exp. Med.* 207: 1247–1260.
42. Zaidi, M. R., and G. Merlino. 2011. The two faces of interferon-γ in cancer. *Clin. Cancer Res.* 17: 6118–6124.
43. Forte, G., A. Rega, S. Morello, A. Luciano, C. Arra, A. Pinto, and R. Sorrentino. 2012. Polyinosinic-polycytidylic acid limits tumor outgrowth in a mouse model of metastatic lung cancer. *J. Immunol.* 188: 5357–5364.
44. Takeda, K., M. Nakayama, M. Sakaki, Y. Hayakawa, M. Imawari, K. Ogasawara, K. Okumura, and M. J. Smyth. 2011. IFN-γ production by lung NK cells is critical for the natural resistance to pulmonary metastasis of B16 melanoma in mice. *J. Leukoc. Biol.* 90: 777–785.
45. Kakuta, S., Y. Tagawa, S. Shibata, M. Nanno, and Y. Iwakura. 2002. Inhibition of B16 melanoma experimental metastasis by interferon-gamma through direct inhibition of cell proliferation and activation of antitumour host mechanisms. *Immunology* 105: 92–100.

Immunobiology 220 (2015) 74–82

Contents lists available at ScienceDirect

Immunobiology

journal homepage: www.elsevier.com/locate/imbio

PolyI:C and mouse survivin artificially embedding human 2B peptide induce a CD4+ T cell response to autologous survivin in HLA-A*2402 transgenic mice

Jun Kasamatsu[a,1], Shojiro Takahashi[a,b,1], Masahiro Azuma[a,1,2], Misako Matsumoto[a], Akiko Morii-Sakai[a], Masahiro Imamura[b], Takanori Teshima[b], Akari Takahashi[c], Yoshihiko Hirohashi[c], Toshihiko Torigoe[c], Noriyuki Sato[c], Tsukasa Seya[a,*]

[a] Department of Microbiology and Immunology, Hokkaido University Graduate School of Medicine, Kita-ku, Sapporo, Japan
[b] Department of Hematology, Hokkaido University Graduate School of Medicine, Kita-ku, Sapporo, Japan
[c] Department of Pathology, Sapporo Medical University School of Medicine, Chuoh-ku, Sapporo, Japan

ARTICLE INFO

Article history:
Received 28 March 2014
Received in revised form 4 August 2014
Accepted 6 August 2014
Available online 23 August 2014

Keywords:
Survivin
PolyI:C
CD4 epitope
Peptide vaccine
Th1 response
Interferon-γ
Tumor immunity

ABSTRACT

$CD4^+$ T cell effectors are crucial for establishing antitumor immunity. Dendritic cell maturation by immune adjuvants appears to facilitate subset-specific $CD4^+$ T cell proliferation, but the adjuvant effect for CD4 T on induction of cytotoxic T lymphocytes (CTLs) is largely unknown. Self-antigenic determinants with low avidity are usually CD4 epitopes in mutated proteins with tumor-associated class I-antigens (TAAs). In this study, we made a chimeric version of survivin, a target of human CTLs. The chimeric survivin, where human survivin-2B containing a TAA was embedded in the mouse survivin frame (MmSVN2B), was used to immunize HLA-A-2402/K^b-transgenic ($HLA24^b$-Tg) mice. Subcutaneous administration of MmSVN2B or xenogeneic human survivin (control HsSNV2B) to $HLA24^b$-Tg mice failed to induce an immune response without co-administration of an RNA adjuvant polyI:C, which was required for effector induction *in vivo*. Although HLA-A-2402/K^b presented the survivin-2B peptide in C57BL/6 mice, 2B-specific tetramer assays showed that no $CD8^+$ T CTLs specific to survivin-2B proliferated above the detection limit in immunized mice, even with polyI:C treatment. However, the $CD4^+$ T cell response, as monitored by IFN-γ, was significantly increased in mice given polyI:C + MmSVN2B. The Th1 response and antibody production were enhanced in the mice with polyI:C. The CD4 epitope responsible for effector function was not $Hs/MmSNV_{13\text{-}27}$, a nonconserved region between human and mouse survivin, but region 53-67, which was identical between human and mouse survivin. These results suggest that activated, self-reactive $CD4^+$ helper T cells proliferate in MmSVN2B + polyI:C immunization and contribute to Th1 polarization followed by antibody production, but hardly participate in CTL induction.

Introduction

Dendritic cells (DCs) present exogenous antigens (Ags) to cells in the major histocompatibility complex (MHC) class I-restricted Ag-presentation pathway and cause the proliferation of $CD8^+$ T cells specific to the extrinsic Ag. When tumor cells have soluble and insoluble exogenous Ags, MHC class I Ag presentation is mainly transporter associated with antigen processing (TAP)- and proteasome-dependent, suggesting the pathway is partly shared with the pathway for endogenous Ag presentation. The delivery of exogenous Ag by DCs to the pathway for MHC class I-restricted Ag presentation is called cross-presentation (Bevan 1976).

PolyI:C is a double-stranded RNA analog that activates RNA-sensing pattern-recognition receptor pathways (Matsumoto and Seya 2008; Seya and Matsumoto 2009). PolyI:C is an efficient trigger of cross-presentation, and facilitates cross-priming of $CD8^+$ T cells in the presence of Ag. Tumor-associated antigens (TAAs) usually expressed in low levels are thought to need support from pattern-recognition receptor activation to induce TAA-specific cytotoxic T lymphocytes (CTLs) (Seya et al. 2013).

* Corresponding author at: Department of Microbiology and Immunology, Hokkaido University Graduate School of Medicine, Kita 15, Nishi 7, Kita-ku, Sapporo 060-8638, Japan. Tel.: +81 11 706 7866; fax: +81 11 706 7866.
E-mail address: seya-tu@pop.med.hokudai.ac.jp (T. Seya).
[1] These authors equally contributed.
[2] Present address: University of Montreal, 2900 Edouard-Montpetit, Faculty of Medicine/Pavilion Roger Gaudry, Department of Pathology and Cellular Biology, Montreal, QC, H3T 1J4, Canada.

http://dx.doi.org/10.1016/j.imbio.2014.08.017
0171-2985/

Many TAAs have been identified and tested for tolerability to patients and for ability to suppress tumor progression. Peptide vaccine immunotherapy against cancer has been studied clinically (Rosenberg et al. 2004). Survivin (SVN) is a TAA that generates CTLs in cancer patients (Schmitz et al. 2000; Andersen et al. 2001). Human survivin (HsSVN) is a 16.5 kDa cytoplasmic protein that inhibits caspase 3 and 7 in cells stimulated to undergo apoptosis (Altieri 2001). SVN is a member of the inhibitor of apoptosis protein family associated with fetal development. Therefore, except for testis, thymus and placenta, normal tissues express little SVN (Ambrosini et al. 1997; Altieri 2001). SVN is required in early thymocyte development from CD4/CD8-double-negative cells to CD4/CD8-double-positive lymphocytes (Okada et al. 2004). SVN is expressed in a wide variety of malignant cells (Altieri 2001; Fukuda and Pelus 2006). There are several splicing variants including a variant HsSVN2B with a cryptic epitope for MHC class I in humans. An HsSVN2B peptide (AYACNTSTL: 80–88) is an HLA-A*2402-restricted peptide recognized by CD8+ CTLs (Hirohashi et al. 2002). Some cancer cells have higher mRNA levels of the HsSVN splice variant 2B, but whether this splice variant functions in tumorigenesis is unknown (Li 2005).

Several trials have studied the SVN2B peptide in cancer patients (Tsuruma et al. 2008; Honma et al. 2009; Kameshima et al. 2013). Although CTLs specific for SVN were detected in peripheral blood mononuclear cells of most cancer patients, as determined by HLA-A*2402/SVN2B tetramer assays, no substantial therapeutic effect on cancer is seen in most clinical studies. A phase I clinical study found that vaccination with SVN2B peptide combined with IFN-α had significant therapeutic benefits in advanced pancreatic cancer patients, in spite of IFN-mediated side effects. Thus, an IFN-inducing adjuvant, that simultaneously up-regulates Ag-presentation and IFN-inducible genes, might more efficiently contribute to the clinical benefits of SVN for cancer patients.

PolyI:C is an analog of virus double-stranded RNA with IFN-inducing adjuvant properties. To test the effect of polyI:C on survivin-derived CTLs, we used a mouse model expressing human HLA-A24 that presents the SVN2B peptide (Gotoh et al. 2002). Mice have no splice counterpart for HsSVN2B and therefore mouse survivin (MmSVN) lacks the 2B portion of HsSVN, although the mouse ortholog is 84% homologous to HsSVN (Kobayashi et al. 1999). When BALB/c mice are injected intraperitoneally with HsSVN2B + RNA adjuvant, high levels of $CD4^+$ T cells are induced in splenic T cells, as determined by IFN-γ, TNF-α, and IL-2 production, as well as development of lytic MHC class II-restricted T cells and memory (Charalambous et al. 2006).

The N-terminal sequence of HsSVN, which includes amino acids 13–27 (FLKDHRISTFKNWPF), differs from that of MmSVN (YLKNYRIATFKNWPF) (Charalambous et al. 2006). Therefore, high frequencies of self-reactive $CD4^+$ T cells specific for a tumorigenic protein might be elicited in mice with xenogeneic HsSVN. However, self-reactive $CD4^+$ T cells can be induced toward syngeneic or nonmutated CD4 epitopes in cancer patients (Topalian et al. 1996; Osen et al. 2010). To test the possibility that sub-derived self-CD4 epitopes participate in $CD8^+$ CTL proliferation, we made a chimeric survivin protein (MmSVN2B), where the human 2B exon sequence was embedded into MmSVN. We immunized HLA-A-2402/K^b-transgenic ($HLA24^b$-Tg) B6 mice with MmSVN2B. The results indicated that the $CD8^+$ CTL response to a self-tumor Ag (2B peptide) was barely enhanced by treatment of $HLA24^b$-Tg mice with MmSVN2B in the presence of polyI:C. However, $CD4^+$ T cell immune responses to the CD4 epitope of MmSVN2B and HsSVN2B were significantly enhanced in $HLA24^b$-Tg mice with SVN2B proteins + polyI:C. The CD4 epitopes were not the N-terminal $HsSVN_{13-27}$ and $MmSVN_{13-27}$ sequences, but the $Hs/MmSVN_{53-67}$ (DLAQCFFCFKELEGW) sequence, which is identical in HsSVN2B and MmSVN2B and thus a nonmutated CD4 epitope. PolyI:C was required for proliferation of self-reactive $CD4^+$ Th1 cells that recognized the syngeneic epitope. We discuss how RNA adjuvant might induce $CD4^+$ Th1 cells and act in the antitumor immune response.

Materials and methods

Bioinformatics analysis

Ensembl databases (http://asia.ensembl.org/index.html) were used to investigate human and mouse SVN genomic structure. Primate and rodent short interspersed nuclear elements (SINEs) were predicted using the Repeat Masker program (http://www.repeatmasker.org/). Results from databases were confirmed by comparison to previous reports (Mahotka et al. 1999).

Expression analysis

Total RNA was extracted from tissues from C57BL/6 mice and murine cell lines using RNeasy Mini Kits (Qiagen) following the manufacturer's instructions. RT-PCR used High Capacity cDNA Reverse Transcription Kits (Applied Biosystems) according to the manufacturer's instructions. Primer pairs were designed to span separate exons to avoid amplifying other genomic DNA. Primers were 5′-ACTACCGCATCGCCACCT-3′ (forward) and 5′-GCTTGTTGTTGGTCTCCTTTG-3′ (reverse) for detection of the murine SVN gene (MmSVN) and 5′-TGTAACCAACTGGGACGATAT-3′ (forward) and 5′-CTTTTCACGGTTGGCCTTAG-3′ (reverse) for murine *Gapdh*. PCR conditions for mSVN were 94 °C 3 min; 35 cycles of 94 °C 30 s, 65 °C 30 s, 72 °C for 30 s; and 7 min 72 °C. *Gapdh* PCR conditions were 94 °C 3 min; 30 cycles of 94 °C 30 s, 65 °C 30 s, and 72 °C 30 s; and 7 min at 72 °C.

Antigens

The HsSVN2B-coding sequence was amplified using primers 5′-CGGGATCCATGGGTGCCCCGACG-3′ (underline: *Bam*HI site) and 5′-GGAATTCTCAATCCATGGCAGC-3′(underline: *Eco*RI site). To construct the mSVN 2B gene (MmSVN2B), we used two-step PCR to make a chimeric gene of the mSVN gene and the human 2B exon (Fig. 2). In the first PCR, two fragments containing exon 1–2 and exon 3–4 were amplified using primers 5′-CCGCTCGAGATGGGAGCTCCGGCGCT-3′ (underline: *Xho*I site) and 5′-*ACCGTGCCCGGCCCA*ATCGGGTTGTCA-3′ (italics: 5′-end of exon 2B of the HsSVN2B gene) for exon 1 and exon 2 and 5′-*GGGCGGATCACGAG*AGAGGAGCATAGAAAGCA-3′ (italics: 3′-end of exon 2B) and 5′-CGGGATCCTTAGGCAGCCAGCTGCTCAAT-3′ (underline: *Bam*HI site) for exon 3 and exon 4. The exon 2B fragment was amplified using primers 5′-*CGATGACAACCCGATT*GGGCCGGGCACGG-3′ (italics: 3′-end of exon 1 and exon 2 of MmSVN) and 5′-*TTTCTATGCTCCTCT*CTCGTGATCCGCCC-3′ (italics: 5′-end of exon 3 and exon 4 of MmSVN). In the second PCR, the three templates from the first PCR were mixed in equal amounts and amplified using primers 5′-CCGCTCGAGATGGGAGCTCCGGCGCT-3′ (underline: *Xho*I site) and 5′-CGGGATCCTTAGGCAGCCAGCTGCTCAAT-3′ (underline: *Bam*HI site). The pCold vector II (TaKaRa) and SVN fragments were restriction digested and ligated overnight with T4 ligase (Promega) at 4 °C. Ligation mixtures were transformed into competent *Escherichia coli* strain BL21 (DE3) cells. After preculturing for 2 h at 37 °C, cells were cooled on ice. Recombinant protein expression was induced with isopropyl-1-thio-β-D-galactopyranoside at a final concentration of 1 mM and cultured for 24 h at 16 °C. N-His-tagged survivin proteins were purified using a Profinia protein purification system (Biorad). Buffer of

purified SVN proteins was sequentially exchanged with PBS containing 2 M urea. To rule out lipopolysaccharide contamination, we treated survivin proteins with 200 μg/ml of polymixin B (Sigma) for 30 min at 37 °C before use. OVA (ovalbumin) (Sigma) was similarly treated with polymixin B as an Ag.

Mice

C57BL/6 (H-2b) mice were from Clea Japan (Tokyo). HLA24^b-Tg was from SLC Japan (Gotoh et al. 2002). Mice were maintained in the Hokkaido University Animal Facility (Sapporo, Japan) in specific pathogen-free conditions. All experiments used mice that were 8–12 weeks old at the time of first procedure. All mice were used according to the guidelines of the institutional animal care and use committee of Hokkaido University, which approved this study (ID number: 08-0243, "Analysis of immune modulation by toll-like receptors").

Reagents, antibodies and cells

PolyI:C and $OVA_{323-339}$ peptide (ISQAVHAAHAEINEAGR) were from Sigma. $OVA_{257-264}$ peptide (SIINFEKL: SL8), OVA (H2 K^b-SL8), HLA-A*2402 survivin-2B and HIV tetramer were from MBL. SVN2B peptide (AYACNTSTL) and HLA-A*2402/2B peptide-restricted human T cell clones (Idenoue et al. 2005) were kindly provided by Dr. Noriyuki Sato (Department of Pathology, School of Medicine, Sapporo Medical University). Human and murine-specific helper peptides (Charalambous et al. 2006) $MmSVN_{13-27}$ (YLKNYRIATFKNWPF) and Hs SVN_{13-27} (FLKDHRISTFKNWPF) and the common helper peptide Hs/Mm SVN_{53-67} (DLAQCFFCFKELEGW), were synthesized by Biologica Co. Ltd (Nagoya). Peptide purity was >95%. To eliminate lipopolysaccharide contamination, all peptides were treated with 200 μg/ml polymixin B (Sigma) for 30 min at 37 °C before use (Nishiguchi et al. 2001). Anti-CD3ε (145-2C11), anti-CD8α (53-6.7) and anti-IFNγ (XMG1.2) antibodys (Abs) were from BioLegend. Anti-CD4 Ab (L3T4) was from eBiosciences and ViaProbe was from BD Biosciences. Dendritic cells were prepared from spleens of mice as described previously (Azuma et al., 2012).

Antigen-specific T cell expansion in vivo

HLA24^b Tg mice (Gotoh et al. 2002) were subcutaneously immunized with 100 μg of each antigen and 100 μg poly I:C once a week for 4 weeks. After 7 days from the last immunization, spleens were extracted, homogenized and stained with FITC-CD8α and PE-OVA (Azuma et al. 2012) or PE-SVN2B tetramer for detecting antigen-specific CD8$^+$ T cells (Tsuruma et al. 2008). For intracellular cytokine detection, splenocytes were cultured with 100 nM SL8 or survivin 2B peptide for 6 h with 10 μg/ml brefeldin A (Sigma–Aldrich) added in the last 4 h. For intracellular cytokine detection of antigen-specific CD4$^+$ T cells, splenocytes were cultured with 100 nM $OVA_{323-339}$ peptide or SVN helper peptide for 6 h with 10 μg/ml brefeldin A (Sigma–Aldrich) added in the last 5 h. Cells were stained with PE-anti-CD8α/FITC-anti-CD3ε for CD8$^+$ T cells or PE-anti-CD4/FITC-anti-CD3ε for CD4$^+$ T cells. After cell-surface staining, cells were fixed and permeabilized with Cytofix/Cytoperm (BD Biosciences) according to the manufacturer's instruction. Fixed and permeabilized cells were stained with APC-anti-IFN-γ. Stained cells were analyzed with FACSCalibur (BD Biosciences) and FlowJo software (Tree Star) (Azuma et al. 2012).

ELISA

Sera were collected from immunized mice once a week for 4 weeks and 96-well plates were coated with 10 μg/ml OVA, MmSVN2B and HsSVN2B in ELISA/ELISPOT coating buffer (eBioscience) and incubated overnight at 4 °C. ELISA diluent solution (eBioscience) was used for blocking and antibody dilution. PBS with 0.05% Tween 20 was used for washes. Anti-OVA or anti-SVN in sera was assessed by ELISA using antiserum for IgG2a/b and IgG1 diluted 1000-fold and 10,000-fold and incubated for 2 h at room temperature. After washing, isotype IgGs were detected using goat anti-mouse total IgG, IgG1, or IgG2a conjugated to HRP (Southern Biotechnology Associates). After washing, plates were stained with 1XTMB ELISA substrate solution (eBioscience) and reactions stopped with 2 N H_2SO_4 before measuring absorbance.

Statistical analyses

For comparison of two groups, *P*-values were calculated with a Student's *t*-test. For comparison of multiple groups, P-values were calculated with one-way analysis of variance (ANOVA) with Bonferroni's test. Error bars are SD or SEM between samples.

Results

Origin of human SVN exon 2B

The HsSVN gene has four conserved and two cryptic exons (Mahotka et al. 1999). The authentic HsSVN gene encode 142 amino acids in exons 1–4. On the other hand, the HsSVN2B product is 165 amino acids encoded by exons 1, 2, 2B, 3 and 4. Exon 2B is hidden within intron 2, which is spliced into mature HsSVN2B mRNA in-frame between exons 2 and 3 (Mahotka et al. 1999). Exon 2B is followed by the GT-AG role and expressed in many tumor cells and tumor cell lines, suggesting that splicing predominantly occurs in malignantly transformed cells (Mahotka et al. 2002). According to the Ensembl database, HsSVN intron 2 had two Alu sequences (Fig. 1A), and exon 2B resulted from the second Alu. In contrast, the MmSVN gene had four exons separated by three introns with no Alu sequence in intron 2; instead, MmSVN had several SINE sequences characteristic of rodents in intron 2 (Fig. 1A). Although the exon sequences were conserved in human and mouse SVNs, two intron sequences diverged between human and mouse (Fig. 1A). These results suggested that integration of exon 2B was evolutionarily new and formed after an Alu insertion. Although the SVN gene is conserved in yeast and humans, exon 2B was established after the divergence of human and mouse.

We used RT-PCR to investigate transcripts resulting from splicing other exons around exon 2 into the MmSVN mRNA. Results of mRNAs from mouse organs and cell lines are in Fig. 2B. The results suggested that no alternative exons around exon 2 in the MmSVN gene. We detected a ~200 bp product in most organs and cell lines tested (Fig. 2B), but this was not an MmSVN transcript.

Generation of a mmSVN2B construct

A SVN2B peptide derived from the HsSVN2B gene that contained the exon 2B sequence was recognized by CTLs in cancer patients (Hirohashi et al. 2002; Tsuruma et al. 2008; Honma et al. 2009) and a CTL clone was established from patients (Idenoue et al. 2005). We artificially constructed an MmSVN2B with a xenogeneic human exon 2B inserted into the boundary between exon 2 and 3 of SVN (Fig. 2A and B). Prominent amino acid substitutions between MmSVN2B and HsSVN2B were concentrated in the N-terminal region encoded by exon 1 (Fig. 2B), and a CD4 epitope is in this region (Li 2005; Mahotka et al. 2002). In an earlier paper, this $HsSVN_{13-27}$ region, but not $MmSVN_{13-27}$, was an effective CD4 epitope that promoted $HsSVN_{13-27}$-specific CD4$^+$ T cell proliferation

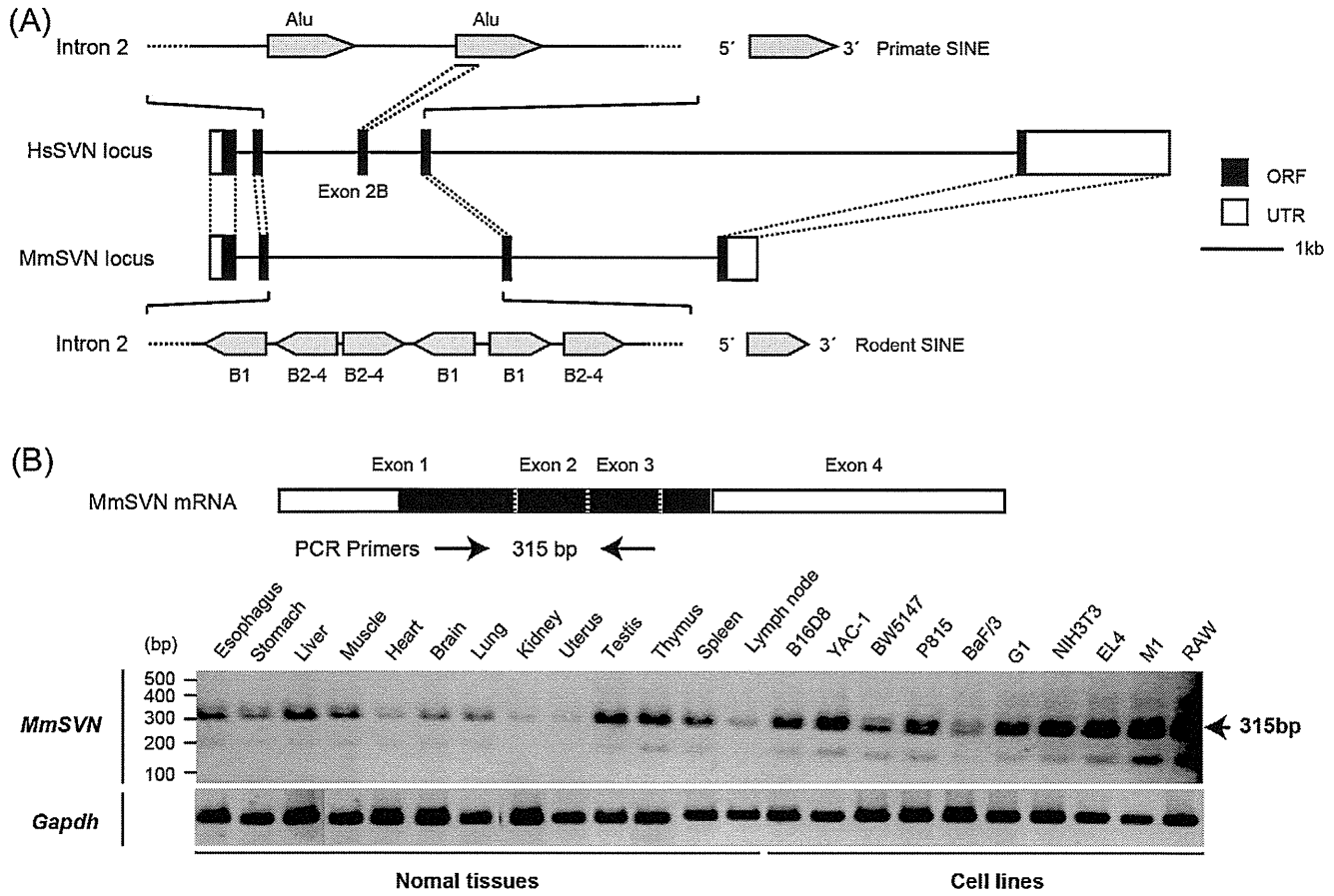

Fig. 1. Genome structure and expression of human and murine SVN gene. (A) Comparison of human and murine survivin gene structure. Survivin gene structures were defined by the Ensembl genome browser. Primate and rodent SINEs were predicted using Repeat Masker program. Filled boxes, coding regions; open boxes, 5′- and 3′-untranslated regions. (B) Structure of murine survivin transcript and RT-PCR analysis of organs and cell lines. Arrows, survivin-detecting PCR primers.

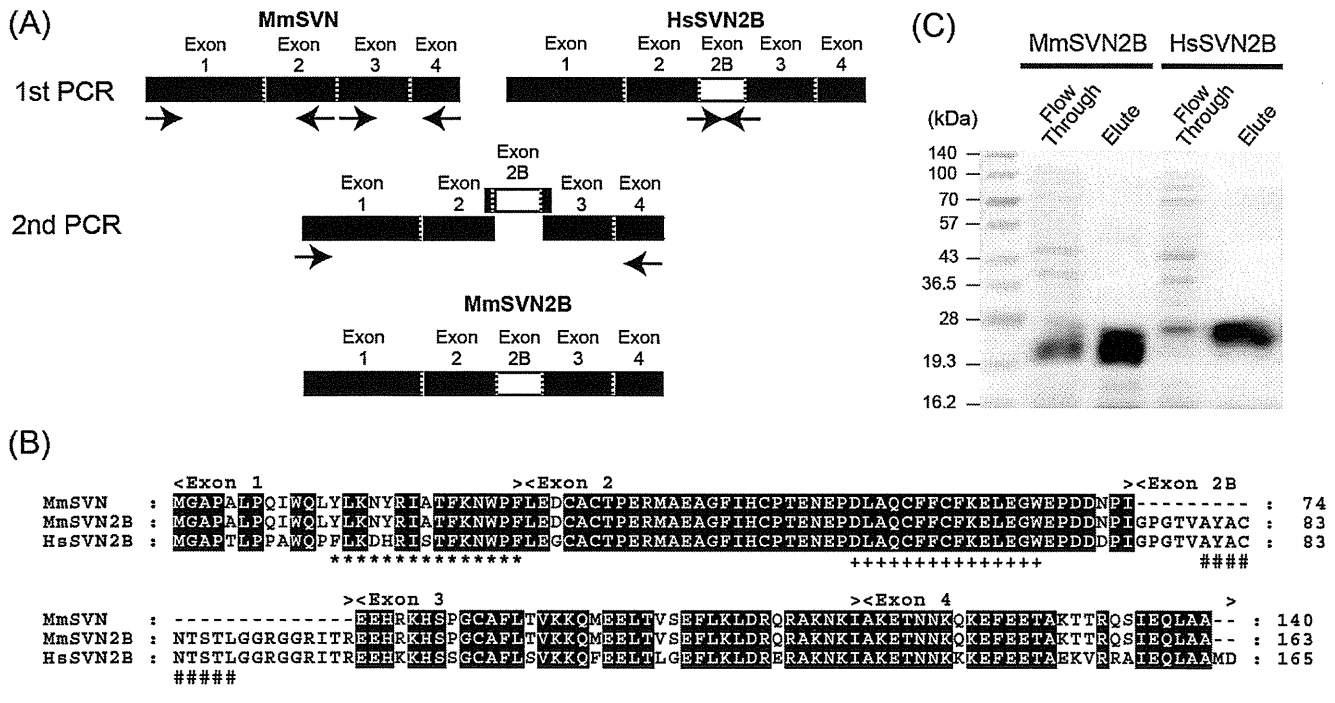

Fig. 2. Structure and purification of chimeric MmSVN2B protein. (A) Strategy for constructing chimeric MmSVN2B protein. Human exon 2B was inserted into MmSVN by PCR. (B) Alignment of murine and human SVN sequences. Black shaded area, residues conserved between human and murine SVN; Hs, human; Mm mouse. *, $MmSVN_{13\text{-}27}$/$HsSVN_{13\text{-}27}$ peptide; +, Hs/Mm $SVN_{53\text{-}67}$ peptide; #, SVN2B peptide. (C) Purification of N-His-tagged MmSVN2B and HsSVN2B proteins. N-His-tagged SVN proteins were purified using a Profinia protein purification system from BL21 (DE3) competent cells. Purified SVN protein buffer was sequentially exchanged to PBS containing 2 M urea.

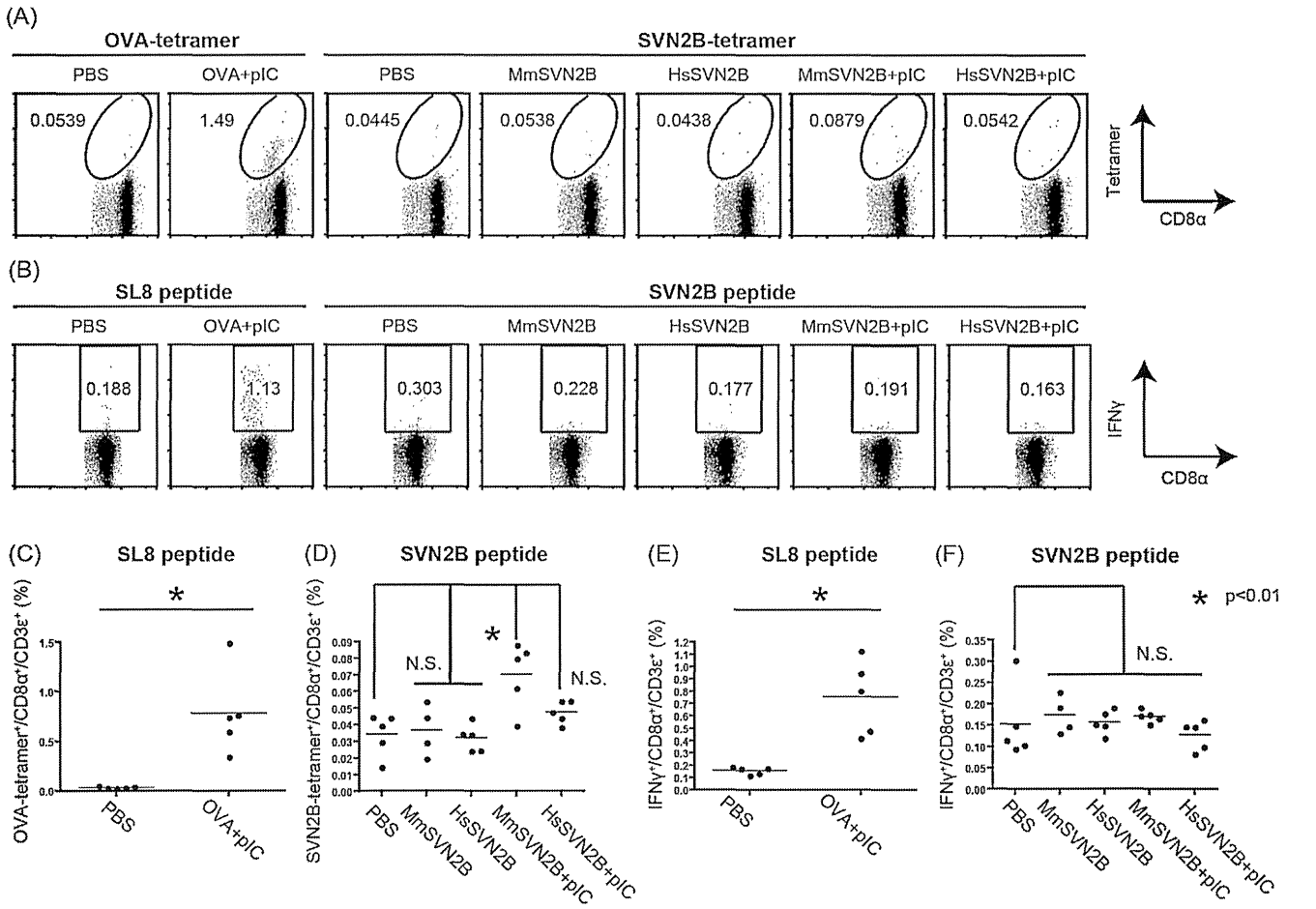

Fig. 3. Expansion of OVA and SVN-specific CD8$^+$ T cells. (A) HLA24^b-Tg mice were immunized with 100 μg antigen and 100 μg poly I:C once a week for 4 weeks. After 7 days from the last immunization, spleens were homogenized and stained with FITC-CD8α and PE-OVA or PE-survivin tetramer to detect antigen-specific CD8$^+$ T cells. (B) Splenocytes were cultured *in vitro* in the presence of SL8 or SVN2B peptides for 6 h and IFN-γ production was measured by FACS. (C, D) Average percentages of OVA-positive and SVN2B-tetramer positive CD8$^+$ T cells shown in (A). (E, F) Average percentages of IFN-γ producing CD8$^+$ T cells specifically in response to SL8 or SVN2B peptide in (B). $^*p < 0.01$.

(Charalambous et al. 2006). His-tagged MmSVN2B and HsSVN2B proteins were purified and used as Ags (Fig. 2C).

CD4$^+$ and CD8$^+$ T cells that react to MmSVN2B plus polyI:C

We examined the ability of MmSVN2B to induce IFN-γ and CD8$^+$ T cell proliferation by immunizing HLA24^b-Tg mice with MmSVN2B or HsSVN2B with or without polyI:C (Fig. 3). SVN2B-specific CTLs were probed by SVN2B-tetramer (Fig. 3A) and IFN-γ staining (Fig. 3B). SVN2B-specific human CD8$^+$ T cells were detected with SVN2B-tetramer (Fig. S1), which enabled us to search for SVN2B-specific CTLs in HLA24^b-Tg mice (Idenoue et al. 2005). Expression of CD40 was up-regulated in CD8α$^+$ conventional DCs to a similar extent with MmSVN2B or HsSVN2B (Fig. S2), consistent with a report on CD40 that promotes cross-priming by Ahonen et al. (J Exp Med, 2004). OVA and polyI:C were used as positive controls (Fig. 3A, B left panels), and SL8 (SIINFEKL)-specific CTLs were monitored with OVA tetramer (Azuma et al. 2012). Both OVA-tetramer-positive and IFN-γ-producing CD8$^+$ T cells were detected in mice immunized with OVA and polyI:C (Fig. 3C, E). Without polyI:C stimulation, only small number of OVA-tetramer-positive cells were upregulated compared to controls (Azuma et al. 2012; Azuma & Seya unpublished data).

When HLA24^b-Tg mice were immunized with MmSVN2B or HsSVN2B without polyI:C, no significant induction of SVN2B-tetramer-positive (Fig. 3D) or IFN-γ-inducing cells was observed (Fig. 3F). When polyI:C was included, only a small increase in SVN2B-tetramer-positive cells was detected in mice given MmSVN + polyI:C with no significant increase in IFN-γ (Fig. 3F). Mice receiving HsSVN + polyI:C (Fig. 3D) or polyI:C alone (not shown) showed no significant increase in SVN2B-specific CD8$^+$ T cells. Consistent with the lack of tetramer-positive CTL induction, MmSVN2B treatment failed to regress MmSVN2B-transfected tumor cells implanted into HLA24^b-Tg mice. In EG7 tumor-bearing mice, administration of polyI:C alone (without Ag) induces tumor-growth retardation due to the contribution of endogenous Ag (Azuma et al. 2012), but in this case with tumor-unloaded mice polyI:C exhibited no tumor-regressing activity (data not shown), possibly due to the lack of Ag.

Next, we determined the amounts of CD4$^+$ T cells that reacted with MmSVN2B. The positive control group received OVA Ag and polyI:C (Fig. 4A, B). The negative control group received PBS without Ag and polyI:C, but basal frequencies of IFN-γ-producing CD4$^+$ T cells were detected in this group even in the absence of polyI:C or Ag (Fig. 4). When MmSVN2B or HsSVN2B only was used to immunize mice, no significant response was seen in CD4$^+$ T cells compared to PBS controls (Fig. 4A, C–E). When polyI:C was included, IFN-γ-producing CD4$^+$ T cells restimulated with Hs/MmSVN$_{53-67}$ peptide increased significantly in mice that received MmSVN and HsSVN (Fig. 4C, D). The sequence of MmSVN$_{53-67}$ was identical to the sequence of HsSVN$_{53-67}$ (Fig. 2B). However, we did not detect a significant increase in IFN-γ-producing CD4$^+$ T cells in mice

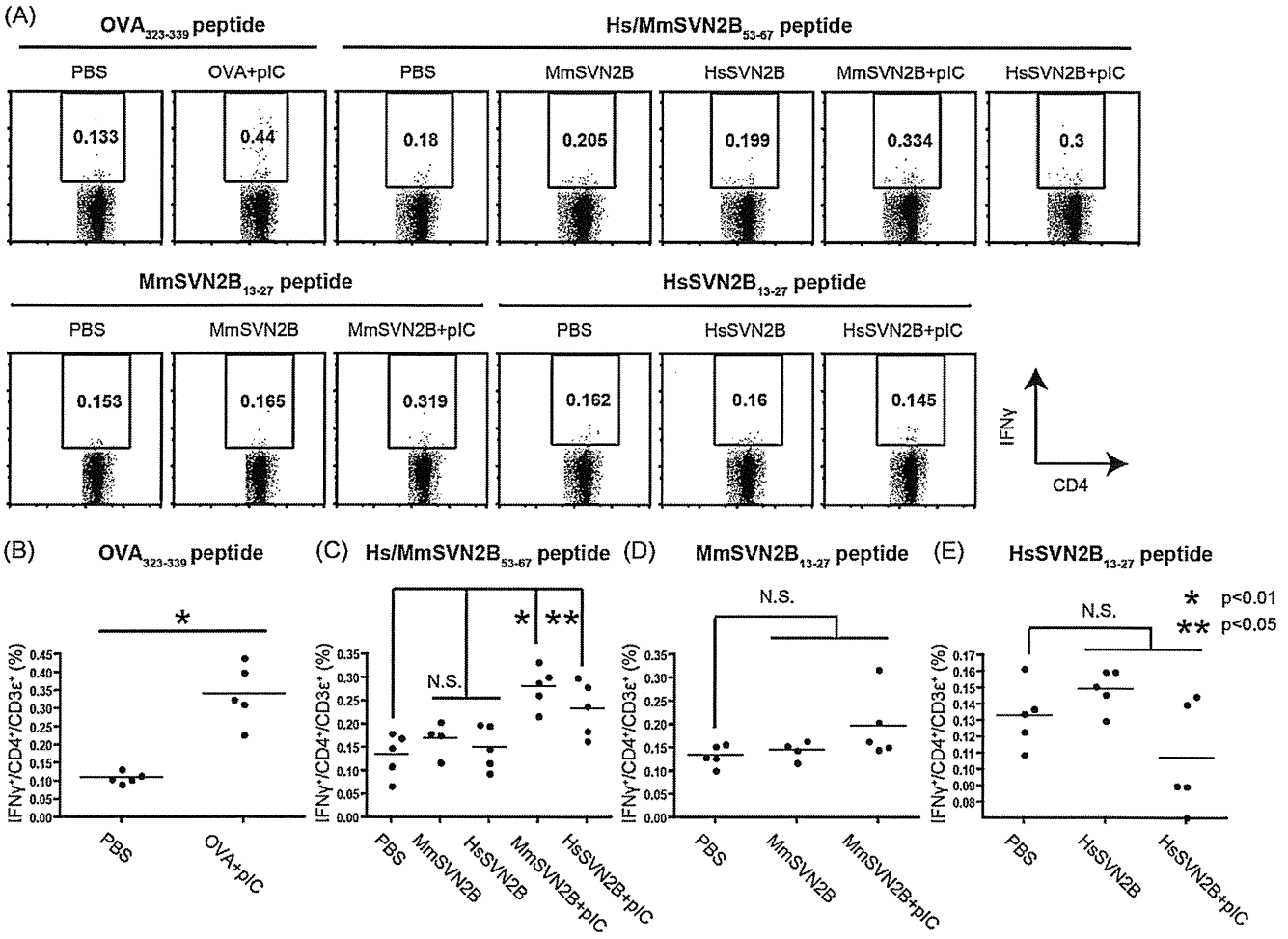

Fig. 4. Expansion of OVA and SVN-specific CD4+ T cells. (A) HLA24b-Tg mice were immunized with 100 μg each antigen and 100 μg poly I:C once a week for 4 weeks. After 7 days from the last immunization, splenocytes were cultured with 100 nM $OVA_{323-339}$ peptide or SVN helper peptide for 6 h, and 10 μg/ml brefeldin A (Sigma–Aldrich) was added in the last 5 h. After cell surface and intracellular staining, IFN-γ production of CD4+ T cells was measured by FACS. Average percentages of IFN-γ-producing CD4+ T cells in response to (B) $OVA_{323-339}$ peptide; (C) Hs/Mm SVN_{53-67} peptide; (D) $MmSVN_{13-27}$ peptide; (E) $HsSVN_{13-27}$ peptide. *$p < 0.01$, **$p < 0.05$.

restimulated with $MmSVN_{13-27}$ or $HsSVN_{13-27}$ peptide (Fig. 4D, E). Differences in these two CD4 epitope sequences are in Fig. 2B.

Ab production by immunization with MmSVN2B with polyI:C

Activation of Th1 cells is essential for B cell antibody class switching. Therefore, we examined production of SVN-specific Ab in Tg mice that did or did not receive polyI:C. Serum was collected from HLA24b-Tg mice immunized with different Ags and polyI:C. OVA and polyI:C were the positive control and resulted in a significant increase in OVA-specific IgG1, IgG2a and IgG2b by ELISA (Fig. 5 left panels). When HLA24b-Tg mice were immunized with MmSVN2B or HsSVN2B without polyI:C, no significant production of any isotypes was observed (Fig. 5 center and right panels). When polyI:C was included, MmSVN2B or HsSVN2B-specific isotypes increased significantly.

Discussion

We demonstrated that HLA24b-Tg mice induced $Hs/MmSVN_{53-67}$-specific CD4+ T cells and SVN-specific Ab followed by Th1 cell activation in response to injection of polyI:C and MmSVN2B protein. This result was partly inconsistent with a previous report (Charalambous et al. 2006) using Balb/c mice and HsSVN conjugated to Dec205 mAb. That is, our study with C57BL/6 mice and MmSVN2B did not detect significant increases in $MmSVN_{13-27}$-specific CD4+ T cells after subcutaneous injection of MmSVN2B with polyI:C. Thus, the xenogeneic differences in sequence between HsSVN and MmSVN did not always contribute to generating effective CD4+ T cells specific for a tumorigenic protein in C57BL/6 mice. The haplotype of the MHC class II proteins between Balb/c (having H-2d) and C57BL/6 mice (having H-2b) and Dec205 mAb conjugation (Charalambous et al. 2006) might be the reason for these different results. However, no CD8+ CTLs against the 2B peptide were detected even when using a specific tetramer for detection of CD8+ CTLs (Fig. S1). Hence, polyI:C was required for proliferation of self-reactive CD4+ Th1 cells that recognized the syngeneic epitope without proliferation of SVN2B peptide-specific CTLs.

OVA were used as positive controls (Fig. 3A, B left panels), and SL8 (SIINFEKL)-specific CTLs were monitored with OVA tetramer (Azuma et al. 2012). Here, T cell activation by polyI:C + MmSVN2B is a focus in this study. However, there is a lot-to-lot difference of T cell-activating activity in polyI:C + OVA as in our present and previous studies (Azuma et al. 2012). This difference of T cell activation may be attributable to the fact that polyI:C consists of a variety of length of polyI chains and polyC chains with a lot-to-lot heterogeneity. In addition, the amounts of Ags in Azuma's experiment are higher than those in the present experiment (Azuma et al. 2012). CD40 stimulation by specific Ab results in high enhancement of cross-priming of CD8 T cells (Charalambous et al. 2006) and CD40 was up-regulated in CD8α+ DCs by polyI:C treatment, but the CD40

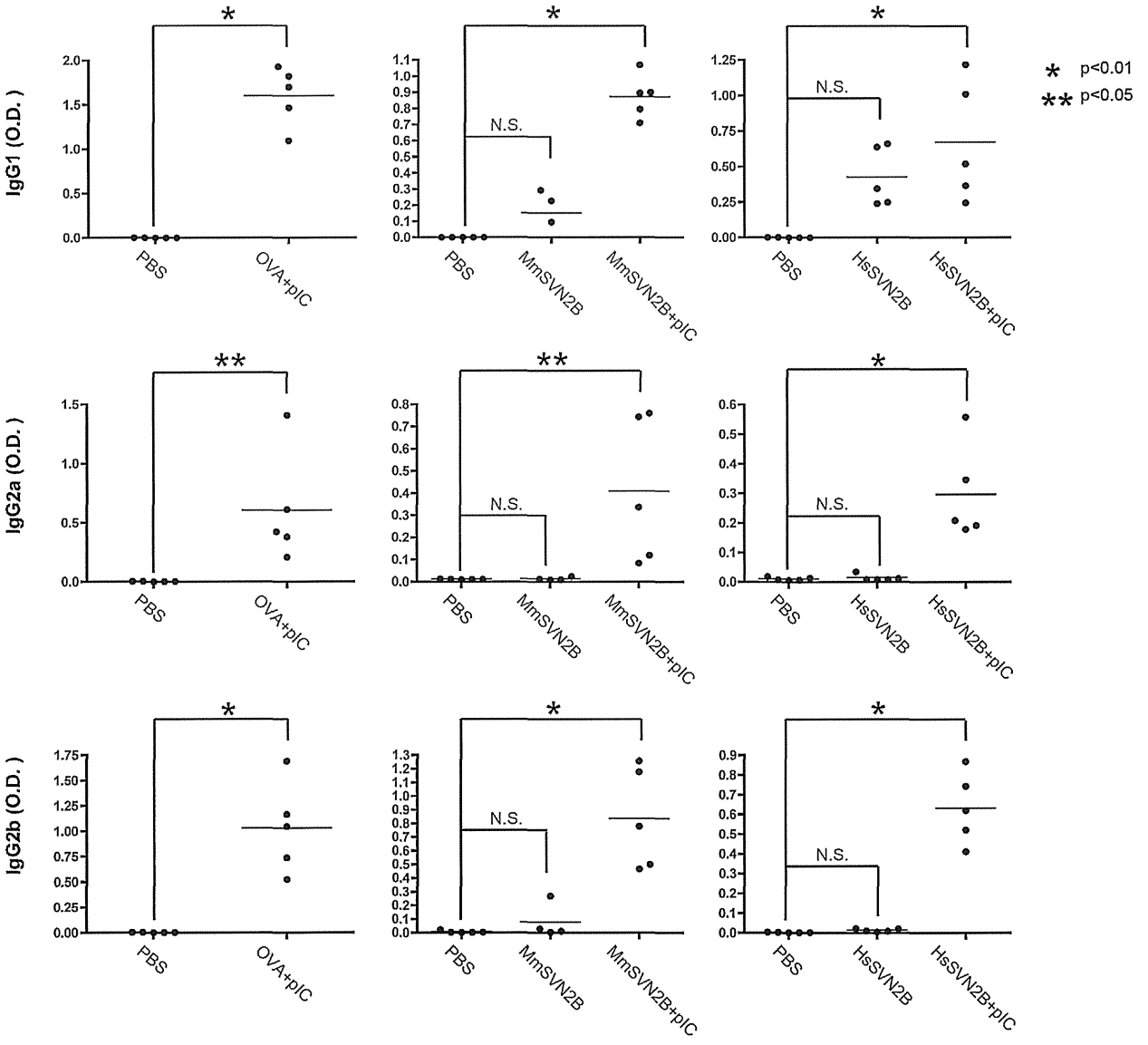

Fig. 5. Production of OVA and SVN-specific antibodies. Sera were collected from immunized mice at once a week for 4 weeks. Anti-OVA or anti-SVN in sera was assessed by ELISA using antiserum for IgG2a/b and IgG1. $^{*}p < 0.01$, $^{**}p < 0.05$.

levels were also variable depending upon the polyI:C lots. Development of a synthesizing method for defined length of RNA duplex will settle the issue.

Two points are noted. First, polyI:C, an RNA adjuvant, induces $CD4^+$ T cells in addition to the reported cases of $CD8^+$ T cells. The factors that participate in polyI:C-mediated CD4+ T cell proliferation and the kind of $CD4^+$ T subsets that are predominantly induced by polyI:C remain unknown. PolyI:C is primarily a potential activator of the IFN-inducing pathways RIG-I/MDA5 and TLR3 (Matsumoto & Seya 2008). These pathways allow host immune cells to produce type I/III IFNs and cytokines and are soluble effectors against cancer. TLR3 preferentially induces cross-presentation in $CD8\alpha^+$ DC in response to dsRNA including polyI:C (Schulz et al., 2005; Azuma et al. 2012) and causes proliferation of $CD8^+$ T cells including cells that respond to TAAs *via* cross-priming (Azuma et al. 2012). $CD4^+$ T cells that are likely evoked by polyI:C stimulation function in antitumor immunity since their helper function is usually suppressed in tumor-bearing mice and can be relieved by innate immune response (Lee et al. 2013). Stimulation with polyI:C + SVN Ag might change a tumor-derived suppressive environment to an environment suitable for primary activation and maintenance of Ag-specific cytotoxic $CD8^+$ T cell responses (Ridge et al. 1998; Janssen et al. 2003).

According to a recent report, however, adoptively transferred $CD4^+$ T cells induce tumor rejection independently of $CD8^+$ T cells (Corthay et al. 2005; Perez-Diez et al. 2007). This rejection is apparently based on cytokines released from $CD4^+$ T cells (Corthay et al. 2005) and on interaction with $CD4^+$ T cells and other immune cells such as macrophages (Mfs) and natural killer (NK) cells (Perez-Diez et al. 2007). DCs stimulated with polyI:C also result in NK cell activation after DC-NK cell-to-cell contact (Akazawa et al. 2007). Mfs in tumors might be a direct target of dsRNA, which converts tumor-supporting Mfs into tumoricidal Mfs (Shime et al. 2012). IL-12p40 is preferentially produced *via* the TICAM-1/Batf3 pathway in response to dsRNA (Azuma et al. 2013). Thus, a variety of cellular effectors can be triggered as antitumor agents by administration of dsRNA with TAA peptides or proteins. We found that $CD4^+$ T cells with Th1 properties were effectors induced by polyI:C possibly acting as an antitumor agent in SVN-responding tumor cells. Although epitope sequence and hydrophobicity might affect Th1 polarization in mice, $CD4^+$ T effectors are successfully induced in tumor-bearing or tumor-implanted mice by stimulation with MmSVN2B + polyI:C.

Hence, *in vivo* administration of an RNA adjuvant with Ag proteins induce $CD4^+$ helper T cells secondary to class II presentation in DCs, together with induction of type I IFNs and cytokines. $CD4^+$ T cells also facilitate Ab production caused by stimulation of B cell development (Mak et al. 2003).

Notably, this is a specific feature of RNA adjuvants, since TLR2 agonist Pam2 lipopeptides such as Pam2CSK4 and MALP2s induce antitumor CTLs with sufficient potential (Chua et al. 2014) but fail to induce DC-mediated antitumor NK cell activation (Yamazaki et al. 2011; Sawahata et al. 2011). $CD4^+$ T cells with regulatory modes such as Tregs and Tr-1 cells and IL-10 were induced by Pam2 peptide in the presence of Ag (Yamazaki et al. 2011). Nevertheless, robust proliferation of antitumor CTL is induced by Pam2 lipopeptides (Chua et al. 2014). Thus, the mode of $CD8^+$ T cell proliferation is differentially modulated between TLR2 and TLR3/MDA5 agonists.

The other point is how self-Ag-reactive $CD4^+$ T cells that act as Th1 effectors in SVN-based immunotherapy are generated. Proliferation of self-reactive T cells is prevented in normal mice, so the levels of self-reactive T cells are usually lower than the detection limit of assays (Gebe et al. 2003). Self-reactive $CD4^+$ T cells might be positively regulated by polyI:C in the presence of protein antigen, since mice, when exposed to DNA/RNA, harbor autoimmune diseases against the protein (Mills 2011). However, even with Ag proteins, polyI:C induced minimal cross-priming of $CD8^+$ T cells in our setting, as with previous reports (Charalambous et al. 2006). In this and other studies, both syngeneic and xenogeneic CD4 epitopes prime $CD4^+$ T cells, stimulating Ab production and Th1 polarization with antitumor activity, but with little association with CTL induction (Charalambous et al. 2006). Our SVN results suggested that self-responsive CD4 epitopes that are identical in sequence in human and mouse SVN have a conserved function as a Th1 skewer, albeit modest, in mice by stimulating DCs and Mfs to prime T and B cells. In this context, however, a question remains to be settled about why the insertion of the 2B sequence in MmSVN caused induction of auto-reactive $CD4^+$ T cells secondary to the class II presentation of the common SVN sequence (53-67) rather than the reported uncommon 13–27 region.

Generally, the presence of Tregs and regulatory cytokines such as IL-10 usually suppresses the function of self-reactive $CD4^+$ T effectors, so an autoimmune response cannot be detected (Danke et al. 2004; Quezada et al. 2010). In tumor-bearing mice, polyI:C releases the restriction of T cell autoreactivity by Tregs to enhance $CD4^+$ T function in a tumor microenvironment. Although the level of Treg cells increases in MALP2s-stimulated tumor-bearing mice (Yamazaki et al. 2011), the amount of Treg cells is not affected by polyI:C injection (Chua et al. 2014). Signs of autoimmune diseases have not yet been observed in mice that received intermittent administration of polyI:C under our conditions. Further studies on the function of regulatory factors in tumor-bearing mice after treatment with various adjuvants are needed to determine the balance between $CD4^+$ T effector functions and regulatory factors including Tregs (Quezada et al. 2010; Corthay et al. 2005).

It has been reported that treatment of murine glioma with DCs loading MmSVN long overlapping peptide covering CD4 and CD8 epitopes (DC therapy) conferred good prognosis on tumor-bearing mice (Ciesielski et al., 2008). In previous trials on peptide vaccine therapy, SVN2B peptide + IFN-α resulted in clinical improvements and enhanced immunological responses of patients (Kameshima et al. 2013). Treatment with SVN2B peptide alone did not result in good prognosis or effective tumor regression in late stage patients with cancer, however (Tsuruma et al. 2008; Honma et al. 2009). These results suggest that both killer and helper T cells are required for *in vivo* induction of tumor regression, as previously suggested (Perez-Diez et al. 2007). NK cells, Mfs, and soluble and angiogenetic factors might be involved in tumor rejection (Shime et al. 2012; Müller-Hermelink et al., 2008; Coussens and Werb 2002) in addition to Ag + polyI:C. According to the study with Ag and polyI:C, a protein or long peptide Ag containing CD4 epitopes, adjuvant RNA and additional factors that disable immunoregulatory factors, are required to effectively induce TAA-specific killer and helper T cell proliferation and subsequent tumoricidal activity in future studies (Casares et al. 2001). Ag peptides should be designed to present both class I and class II peptides on DCs to facilitate proliferation of $CD4^+$ T cells and Ab production. Methods for inducing potential $CD8^+$ CTLs against tumors still need to be considered.

Competing interests

The authors have declared that no competing interest exists.

Acknowledgements

We are grateful to members in our laboratories. JK is a Research Fellow of the Japan Society for the Promotion of Science. This work was supported in part by Grants-in-Aid from the Ministry of Education, Science, and Culture and the Ministry of Health, Labor, and Welfare of Japan, and by a MEXT Grant-in-Project 'the Carcinogenic Spiral', 'the National Cancer Center Research and Development Fund (23-A-44)'. Financial support by the Takeda Science Foundation, the Yasuda Cancer Research Foundation and the Ono Foundation are gratefully acknowledged.

Appendix A. Supplementary data

Supplementary data associated with this article can be found, in the online version, at http://dx.doi.org/10.1016/j.imbio.2014.08.017.

References

Ahonen, C.L., Doxsee, C.L., McGurran, S.M., Riter, T.R., Wade, W.F., Barth, R.J., Vasilakos, J.P., Noelle, R.J., Kedl, R.M., 2004. Combined TLR and CD40 triggering induces potent CD8+ T cell expansion with variable dependence on type I IFN. J. Exp. Med. 199, 775–784.

Altieri, D.C., 2001. The molecular basis and potential role of survivin in cancer diagnosis and therapy. Trends Mol. Med. 7, 542–547.

Akazawa, T., Ebihara, T., Okuno, M., Okuda, Y., Shingai, M., Tsujimura, K., Takahashi, T., Ikawa, M., Okabe, M., Inoue, N., Okamoto-Tanaka, M., Ishizaki, H., Miyoshi, J., Matsumoto, M., Seya, T., 2007. Antitumor NK activation induced by the Toll-like receptor 3-TICAM-1 (TRIF) pathway in myeloid dendritic cells. Proc. Natl. Acad. Sci. U. S. A. 104, 252–257.

Ambrosini, G., Adida, C., Altieri, D.C., 1997. A novel anti-apoptosis gene, survivin, expressed in cancer and lymphoma. Nat. Med. 3, 917–921.

Andersen, M.H., Pedersen, L.O., Becker, J.C., Straten, P.T., 2001. Identification of a cytotoxic T lymphocyte response to the apoptosis inhibitor protein survivin in cancer patients. Cancer Res. 61, 869–872.

Azuma, M., Ebihara, T., Oshiumi, H., Matsumoto, M., Seya, T., 2012. Cross-priming for antitumor CTL induced by soluble Ag + polyI:C depends on the TICAM-1 pathway in mouse CD11c(+)/CD8α(+) dendritic cells. Oncoimmunology 1, 581–592.

Azuma, M., Matsumoto, M., Seya, T., 2013. PolyI:C-derived dendritic cell maturation and cellular effectors depend on TICAM-1-Batf3 axis in mice. Proc. Jpn. Cancer Assoc. 72, 126.

Bevan, M.J., 1976. Cross-priming for a secondary cytotoxic response to minor H antigens with H-2 congenic cells which do not cross-react in the cytotoxic assay. J. Exp. Med. 143, 1283–1288.

Casares, N., Lasarte, J.J., de Cerio, A.L., Sarobe, P., Ruiz, M., Melero, I., Prieto, J., Borrás-Cuesta, F., 2001. Immunization with a tumor-associated CTL epitope plus a tumor-related or unrelated Th1 helper peptide elicits protective CTL immunity. Eur. J. Immunol. 31, 1780–1789.

Charalambous, A., Oks, M., Nchinda, G., Yamazaki, S., Steinman, R.M., 2006. Dendritic cell targeting of survivin protein in a xenogeneic form elicits strong CD4+ T cell immunity to mouse survivin. J. Immunol. 177, 8410–8421, 44.

Chua, B.Y., Olson, M.R., Bedoui, S., Sekiya, T., Wong, C.Y., Turner, S.J., Jackson, D.C., 2014. The use of a TLR2 agonist-based adjuvant for enhancing effector and memory CD8 T-cell responses. Immunol. Cell Biol., http://dx.doi.org/10.1038/icb.2013.102.

Ciesielski, M.J., Kozbor, D., Castanaro, C.A., Barone, T.A., Fenstermaker, R.A., 2008. Therapeutic effect of a T helper cell supported CTL response induced by a survivin peptide vaccine against murine cerebral glioma. Cancer Immunol. Immunother. 57, 1827–1835.

Corthay, A., Skovseth, D.K., Lundin, K.U., Rosjo, E., Omholt, H., Hofgaad, P.O., Haraldsen, G., Bogen, B., 2005. Primary antitumor immune response mediated by CD4+ T cells. Immunity 22, 371–383.
Coussens, L.M., Werb, Z., 2002. Inflammation and cancer. Nature 420, 860–867.
Danke, N.A., Koelle, D.M., Yee, C., Beheray, S., Kwok, W.W., 2004. Autoreactive T cells in healthy individuals. J. Immunol. 172, 5967–6572.
Fukuda, S., Pelus, L.M., 2006. Survivin, a cancer target with an emerging role in normal adult tissues. Mol. Cancer Ther. 5, 1087–1098.
Gebe, J.A., Falk, B.A., Rock, K.A., Kochik, S.A., Heninger, A.K., Reijonen, H., Kwok, W.W., Nepom, G.T., 2003. Low-avidity recognition by CD4+ T cells directed to self-antigens. Eur. J. Immunol. 33, 1409–1417.
Gotoh, M., Takasu, H., Harada, K., Yamaoka, T., 2002. Development of HLA-A2402/K^b transgenic mice. Int. J. Cancer 100, 565–570.
Hirohashi, Y., Torigoe, T., Maeda, A., Nabeta, Y., Kamiguchi, K., Sato, T., Yoda, J., Ikeda, H., Hirata, K., Yamanaka, N., Sato, N., 2002. An HLA-A24-restricted cytotoxic T lymphocyte epitope of a tumor-associated protein, survivin. Clin. Cancer Res. 8, 1731–1739.
Honma, I., Kitamura, H., Torigoe, T., Takahashi, A., Tanaka, T., Sato, E., Hirohashi, Y., Masumori, N., Tsukamoto, T., Sato, N., 2009. Phase I clinical study of anti-apoptosis protein survivin-derived peptide vaccination for patients with advanced or recurrent urothelial cancer. Cancer Immunol. Immunother. 58, 1801–1807.
Idenoue, S., Hirohashi, Y., Torigoe, T., Sato, Y., Tamura, Y., Hariu, H., Yamamoto, M., Kurotaki, T., Tsuruma, T., Asanuma, H., Kanaseki, T., Ikeda, H., Kashiwagi, K., Okazaki, M., Sasaki, K., Sato, T., Ohmura, T., Hata, F., Yamaguchi, K., Hirata, K., Sato, N., 2005. A potent immunogenic general cancer vaccine that targets survivin, an inhibitor of apoptosis proteins. Clin. Cancer Res. 11, 1474–1482.
Janssen, E.M., Lemmens, E.E., Wolfe, T., Christen, U., von Herrath, M.G., et al., 2003. CD4+ T cells are required for secondary expansion and memory in CD8+ T lymphocytes. Nature 421, 852–856.
Kameshima, H., Tsuruma, T., Kutomi, G., Shima, H., Iwayama, Y., Kimura, Y., Imamura, M., Torigoe, T., Takahashi, A., Hirohashi, Y., Tamura, Y., Tsukahara, T., Kanaseki, T., Sato, N., Hirata, K., 2013. *Immunotherapeutic benefit of α-interferon (IFNα) in survivin2B-derived peptide vaccination for advanced pancreatic cancer patients.* Cancer Sci. 104, 124–129.
Kobayashi, K., Hatano, M., Otaki, M., Ogasawara, T., Tokuhisa, T., 1999. Expression of a murine homologue of the inhibitor of apoptosis protein is related to cell proliferation. Proc. Natl. Acad. Sci. U. S. A. 96, 1457–1462.
Lee, M.K.4th, Xu, S., Fitzpatrick, E.H., Sharma, A., Graves, H.L., Czerniecki, B.J., 2013. Inhibition of CD4+CD25+ regulatory T cell function and conversion into Th1-like effectors by a Toll-like receptor-activated dendritic cell vaccine. PLOS ONE 8, e74698.
Li, F., 2005. Role of survivin and its splice variants in tumorigenesis. Br. J. Cancer 92, 212–216.
Mahotka, C., Wenzel, M., Springer, E., Gabbert, H.E., Gerharz, C.D., 1999. Survivin-deltaEx3 and survivin-2B: two novel splice variants of the apoptosis inhibitor survivin with different antiapoptotic properties. Cancer Res. 59, 6097–6102.
Mahotka, C., Liebmann, J., Wenzel, M., Suschek, C.V., Schmitt, M., Gabbert, H.E., Gerharz, C.D., 2002. Differential subcellular localization of functionally divergent surviving splice variants. Cell Death Differ. 9, 1334–1342.
Mak, T.W., Shahinian, A., Yoshinaga, S.K., Wakeham, A., Boucher, L.M., Pintilie, M., Duncan, G., Gajewska, B.U., Gronski, M., Eriksson, U., Odermatt, B., Ho, A., Bouchard, D., Whorisky, J.S., Jordana, M., Ohashi, P.S., Pawson, T., Bladt, F., Tafuri, A., 2003. Costimulation through the inducible costimulator ligand is essential for both T helper and B cell functions in T cell-dependent B cell responses. Nat. Immunol. 4, 765–772.
Matsumoto, M., Seya, T., 2008. TLR3: interferon induction by double-stranded RNA including poly(I:C). Adv. Drug Deliv. Rev. 60, 805–812.
Mills, K.H., 2011. TLR-dependent T cell activation in autoimmunity. Nat. Rev. Immunol. 11, 807–822.
Müller-Hermelink, N., Braumüller, H., Pichler, B., Wieder, T., Mailhammer, R., Schaak, K., Ghoreschi, K., Yazdi, A., Haubner, R., Sander, C.A., Mocikat, R., Schwaiger, M., Förster, I., Huss, R., Weber, W.A., Kneilling, M., Röcken, M., 2008. TNFR1 signaling and IFN-gamma signaling determine whether T cells induce tumor dormancy or promote multistage carcinogenesis. Cancer Cell 13, 507–518.
Nishiguchi, M., Matsumoto, M., Takao, T., Hoshino, M., Shimonishi, Y., Tsuji, S., Begum, N.A., Takeuchi, O., Akira, S., Toyoshima, K., Seya, T., 2001. Mycoplasma *fermentrans* lipoprotein M161Ag-induced cell activation is mediated by Toll-like receptor 2: role of N-terminal hydrophobic portion in its multiple functions. J. Immunol. 166, 2610–2616.
Okada, H., Bakal, C., Shahinian, A., Elia, A., Wakeham, A., Suh, W.K., Duncan, G.S., Ciofani, M., Rottapel, R., Zuniga-Pflucker, J.C., Mak, T.W., 2004. Survivin loss in thymocytes triggers p53-mediated growth arrest and p53-independent cell death. J. Exp. Med. 199, 399–410.
Osen, W., Soltek, S., Song, M., Leuchs, B., Steitz, J., Tüting, T., Eichmüller, S.B., Nguyen, X.D., Schadendorf, D., Paschen, A., 2010. Screening of human tumor antigens for CD4 T cell epitopes by combination of HLA-transgenic mice, recombinant adenovirus and antigen peptide libraries. PLOS ONE 5, e14137.
Perez-Diez, A., Joncker, N.T., Choi, K., Chan, W.F., Anderson, C.C., Lantz, O., Matzinger, P., 2007. CD4 cells can be more efficient at tumor rejection than CD8 cells. Blood 109, 5346–5354.
Quezada, S.A., Simpson, T.R., Peggs, K.S., Merghoub, T., Vider, J., Fan, X., Blasberg, R., Yagita, H., Muranski, P., Antony, P.A., Restifo, N.P., Allison, J.P., 2010. Tumor-reactive CD4(+) T cells develop cytotoxic activity and eradicate large established melanoma after transfer into lymphopenic hosts. J. Exp. Med. 207, 637–650.
Ridge, J.P., Di Rosa, F., Matzinger, P., 1998. A conditioned dendritic cell can be a temporal bridge between a CD4+ T-helper and a T-killer cell. Nature 393, 474–478.
Rosenberg, S.A., Yang, J.C., Restifo, N.P., 2004. Cancer immunotherapy: moving beyond current vaccines. Nat. Med. 10, 909–915.
Sawahata, R., Shime, H., Yamazaki, S., Inoue, N., Akazawa, T., Fujimoto, Y., Fukase, K., Matsumoto, M., Seya, T., 2011. Failure of mycoplasma lipoprotein MALP-2 to induce NK cell activation through dendritic cell TLR2. Microbes Infect. 13, 350–358.
Schmitz, M., Diestelkoetter, P., Weigle, B., Schmachtenberg, F., Stevanovic, S., Ockert, D., Rammensee, H.G., Rieber, E.P., 2000. *Generation of survivin-specific CD8+ T effector cells by dendritic cells pulsed with protein or selected peptides.* Cancer Res. 60, 4845–4849.
Schulz, O., Diebold, S.S., Chen, M., Näslund, T.I., Nolte, M.A., Alexopoulou, L., Azuma, Y.T., Flavell, R.A., Liljeström, P., Reis e Sousa, C., 2005. Toll-like receptor 3 promotes cross-priming to virus-infected cells. Nature 433, 887–892.
Seya, T., Matsumoto, M., 2009. The extrinsic RNA-sensing pathway for adjuvant immunotherapy of cancer. Cancer Immunol. Immunother. 58, 1175–1184.
Seya, T., Azuma, M., Matsumoto, M., 2013. Targeting TLR3 with no RIG-I/MDA5 activation is effective in immunotherapy for cancer. Expert Opin. Ther. Targets 17, 533–544.
Shime, H., Matsumoto, M., Oshiumi, H., Tanaka, S., Nakane, A., Iwakura, Y., Tahara, H., Inoue, N., Seya, T., 2012. Toll-like receptor 3 signaling converts tumor-supporting myeloid cells to tumoricidal effectors. Proc. Natl. Acad. Sci. U. S. A. 109, 2066–2071.
Topalian, S.L., Gonzales, M.I., Parkhurst, M., Li, Y.F., Southwood, S., Sette, A., Rosenberg, S.A., Robbins, P.F., 1996. Melanoma-specific CD4+ T cells recognize nonmutated HLA-DR-restricted tyrosinase epitopes. J. Exp. Med. 183, 1965–1971.
Tsuruma, T., Iwayama, Y., Ohmura, T., Katsuramaki, T., Hata, F., Furuhata, T., Yamaguchi, K., Kimura, Y., Torigoe, T., Toyota, N., Yagihashi, A., Hirohashi, Y., Asanuma, H., Shimozawa, K., Okazaki, M., Mizushima, Y., Nomura, N., Sato, N., Hirata, K., 2008. Clinical and immunological evaluation of anti-apoptosis protein, survivin-derived peptide vaccine in phase I clinical study for patients with advanced or recurrent breast cancer. J. Transl. Med. 6, 24.
Yamazaki, S., Okada, K., Maruyama, A., Matsumoto, M., Yagita, H., Seya, T., 2011. TLR2-dependent induction of IL-10 and Foxp3+ CD25+ CD4+ regulatory T cells prevents effective anti-tumor immunity induced by Pam2 lipopeptides in vivo. PLOS ONE 6, e18833.

HEPATOLOGY
Official Journal of the American Association for the Study of Liver Diseases

Development of Hepatitis C Virus Genotype 3a Cell Culture System

Sulyi Kim,[1] Tomoko Date,[1] Hiroshi Yokokawa,[1,2] Tamaki Kono,[1] Hideki Aizaki,[1] Patrick Maurel,[3] Claire Gondeau,[3,4] and Takaji Wakita[1]

Hepatitis C virus (HCV) genotype 3a infection poses a serious health problem worldwide. A significant association has been reported between HCV genotype 3a infections and hepatic steatosis. Nevertheless, virological characterization of genotype 3a HCV is delayed due to the lack of appropriate virus cell culture systems. In the present study, we established the first infectious genotype 3a HCV system by introducing adaptive mutations into the S310 strain. HCV core proteins had different locations in JFH-1 and S310 virus-infected cells. Furthermore, the lipid content in S310 virus-infected cells was higher than Huh7.5.1 cells and JFH-1 virus-infected cells as determined by the lipid droplet staining area. *Conclusion*: This genotype 3a infectious cell culture system may be a useful experimental model for studying genotype 3a viral life cycles, molecular mechanisms of pathogenesis, and genotype 3a-specific antiviral drug development. (HEPATOLOGY 2014;00:000-000)

About 170 million people worldwide are infected with hepatitis C virus (HCV), which causes chronic liver disease at a high rate, leading to complications including endstage liver disease, liver cirrhosis, and hepatocellular carcinoma.[1] HCV is classified into seven major genotypes.[2] Genotype 1b is the most prevalent HCV genotype in Asian countries, followed by genotype 3a. Genotype 3a infections are more prevalent in South Asian countries with large populations.[3,4] A high incidence of hepatic steatosis is associated with genotype 3a infection.[5-7] Interferon and ribavirin combination therapy is not satisfactory in genotype 3a-infected patients, although it is more effective than in genotype 1b-infected patients.[5] The recently developed protease inhibitors telaprevir and boceprevir are also less effective against genotype 3a infection.[8] New antiviral drug development against genotype 3a HCV is necessary to improve treatment efficiency in genotype 3a-infected patients.

HCV subgenomic replicon systems are useful tools for the study of viral replication mechanisms and antiviral drug development. Recently, genotype 3a replicon systems were established.[9,10] The S310 replicon with adaptive mutations replicated efficiently in cell culture. Genotype 3a infections have a different pathogenesis as compared to other genotype infections (for example, steatosis). Previous studies demonstrated that cells expressing genotype 3a core protein had increased lipid accumulation.[11-13] Therefore, an efficient infectious viral system recapitulating the full life cycle is now essential to determine the precise pathogenesis of genotype 3a infection.

In the present study, we established an infectious genotype 3a HCV cell culture system by using S310 strains. The full-length S310 clones replicated efficiently and produced infectious viral particles. There were different HCV core localization patterns between genotype 3a S310- and genotype 2a JFH-1-infected cells. Interestingly, the lipid content in S310 virus-infected cells was higher than Huh7.5.1 cells and JFH-1 virus-infected cells as determined by lipid droplet staining area. This cell culture system will be very

Abbreviations: DMEM, Dulbecco's Modified Eagle Medium; HCV, hepatitis C virus; IgG, immunoglobulin G; LD, lipid droplet; MOI, multiplicity of infection; RT-PCR, reverse-transcriptase polymerase chain reaction; SGR, subgenomic replicon.

From the [1]Department of Virology II, National Institute of Infectious Diseases, Tokyo, Japan; [2]Pharmaceutical Research Laboratories, Toray Industries, Inc., Kanagawa, Japan; [3]Inserm U1040, Biotherapy Research Institute, Montpellier, France; [4]Department of Hepato-gastroenterology A, Hospital Saint Eloi, CHU Montpellier, France.

Received November 28, 2013; accepted April 29, 2014.

Supported by Grants-in-Aid for Scientific Research from the Japan Society for the Promotion of Science, from the Ministry of Health, Labour and Welfare of Japan, from the Ministry of Education, Culture, Sports, Science and Technology of Japan, and from the Research on Health Sciences Focusing on Drug Innovation from the Japan Health Sciences Foundation.